# 9

### **Review Article**

Linjing Hao, Shenao Wang, Peng Li\*, Yijun Cao and Baolin Xing\*

# Coal-based carbon/graphene quantum dots: formation mechanisms and applications

https://doi.org/10.1515/revic-2024-0071 Received August 12, 2024; accepted October 29, 2024; published online April 3, 2025

Abstract: The Carbon/graphene quantum dots (CQDs/GQDs) have received increasing attention as emerging zerodimensional (0D) carbon nanomaterials. The CODs/GODs were endowed with significant potential in environmental and energy fields, due to the unique photoluminescence, good biocompatibility, excellent electron transfer capability, and low toxicity. Compared with graphite and hydrocarbons, coal and its derivatives are considered as alternative carbon sources for preparing CQDs/GQDs, as their low cost and abundant reserves. Thereby, the important issue of realization the deep processing and functional applications of coal is cracking the C-O bonds that connected the aromatic ring clusters in coal and its derivatives to obtain CODs/ GQDs. This article briefly reviews the synthesis methods and physicochemical properties of coal-based CQDs/GQDs in recent years, focusing on the formation mechanism of coalbased CQDs/GQDs and their functionalization. In addition, their applications in sensing, photocatalysis, electrochemistry and biomedicine are discussed, as well as the prospects for future research. Hopefully, this paper will provide significant support for the design of efficient coal-based carbon nanomaterials and sustainable options for overcoming bottlenecks in coal applications.

\*Corresponding authors: Peng Li, State Key Laboratory of Coking Coal Resources Green Exploitation, School of Chemical Engineering, Zhengzhou University, Zhengzhou 450001, China; and Key Lab of Critical Metals Minerals Supernormal Enrichment and Extraction (Ministry of Education), Zhengzhou University, Zhengzhou 450001, China,

E-mail: zdhglipeng@zzu.edu.cn; and **Baolin Xing**, College of Chemistry and Chemical Engineering, Henan Polytechnic University, Jiaozuo 454003, China, E-mail: baolinxing@hpu.edu.cn

**Linjing Hao and Shenao Wang**, State Key Laboratory of Coking Coal Resources Green Exploitation, School of Chemical Engineering, Zhengzhou University, Zhengzhou 450001, China

**Yijun Cao**, State Key Laboratory of Coking Coal Resources Green Exploitation, School of Chemical Engineering, Zhengzhou University, Zhengzhou 450001, China; and Key Lab of Critical Metals Minerals Supernormal Enrichment and Extraction (Ministry of Education), Zhengzhou University, Zhengzhou 450001, China

**Keywords:** CQDs/GQDs; coal; formation mechanism; functionalization

## 1 Introduction

The Quantum dots (QDs) usually refers to nanoscale particles of conventional semiconductors subject to quantum confinement effects. A number of other nanomaterials with similar redox and optical properties without strictly defined quantum constraints are also referred to as QDs. The semiconductor QDs has been used for many years in applications, such as bioimaging and sensing, owing to their tunable fluorescence emission properties and quantum confinement effects.<sup>2-4</sup> However, the semiconductor QDs is highly toxic as heavy metals are used in the production process, such as mercury, lead and cadmium, limiting their commercial large-scale production. 5,6 In order to overcome the toxicity of heavy metal ions, the carbon dots (CDs) was emerged as an alternative. The CDs was firstly discovered during the purification of single walled carbon nanotubes (SWNTs) by Xu et al. in 2004, reported and described as carbon nanoparticles (CNPs). Subsequently, the CDs attracted the interest of researchers due to their excellent structural features and physicochemical properties. Compared with conventional semiconductor QDs, the CDs has the advantages of low cost, low toxicity, abundant sources, good biocompatibility and simple preparation process.<sup>8,9</sup> Additionally, luminescence properties and photophysical properties are important properties of CDs. Currently, the CDs has been demonstrated to wide range of luminescence types and photophysical properties, such as fluorescence (FL), phosphorescence, electroluminescence (EL), tunable emission wavelength, and high photoluminescence quantum yield. 10-19 These properties have led to widespread applications of CDs in catalysis, batteries, bioimaging, and biosensing.<sup>20–28</sup> They are connected to each other by changing the degree of carbonisation or graphene layer to establish connections. Two methods have been proposed for synthesizing CDs, namely "bottom-up" and "top-down". 29-31 The "bottom-up" mainly uses microwave or hydrothermal methods to synthesise CDs from molecular precursors.

However, the process is more complicated and the reactive precursors are limited.<sup>32</sup> The "top-down" uses arc discharge, laser ablation, or chemical oxidation to decompose and strip carbon-containing materials, which is simple and has a relatively large number of reactants. However, the preparation process of pristine carbon precursors, like carbon fibres, carbon nanotubes, fullerenes, and graphite, used for this method is more complicated and expensive, which has impeded the practical applications and large-scale production of CDs. Therefore, the development of low-cost precursors for carbon nanomaterials is a very interesting study.

Coal is the most widely distributed and abundant fossil fuels on earth.<sup>33</sup> The "Peak Carbon and Carbon Neutral" target has ushered the world into an era of climate economy, creating opportunities and challenges for green transformation. More and more countries have started to reduce the share of coal in their energy mix in order to reduce greenhouse gas emissions.<sup>34</sup> Therefore, low-carbon processing and clean utilisation of coal is one of the key issues that need to be researched nowadays. Coal is a natural nonhomogeneous polymeric material with a three-dimensional crosslinked structure consisting of a certain number of hydrogen-aromatic and aromatic units attached by macromolecular structures and bridge bonds. 35,36 Additionally, coal can be turned into chemical products such as liquid fuels, coal tar, coke and coal pitch through catalytic processing and thermal processing. These coal derivatives maintain the structural characteristics of coal. Thereby, it is an effective way to construct coal-based carbon materials by using coal as well as its derivatives as carbonaceous precursors. The feasibility of preparing fullerenes from coke was first demonstrated by Pang et al. in 1991.<sup>37</sup> Since then, more and more researches have been focused on synthesizing coal-based carbon materials such as carbon nanofibres, 38,39 carbon nanosheets, 40-42 diamond, 43 carbon nanoparticles, 44-46 porous carbon materials, 47,48 graphene, graphene oxide, <sup>49–51</sup> and more recently CDs. Coal-based CDs usually have tunable light trapping ability, excellent electron transfer efficiency, abundant surface active sites and functional groups, and are used in a variety of applications including batteries, sensing, catalysis and bioimaging. The coal-based CDs is mainly classified into graphene quantum dots (GQDs) and carbon quantum dots (CQDs), based on their structure, formation mechanisms, and properties. CODs are quasi-spherical nanoparticles with diameters of 2-10 nm, containing mainly sp3 hybridised carbon, and have good solubility in various solvents. GQDs, on the other hand, are usually graphene fragments with diameters below 20 nm small enough to induce quantum size effects, and are mainly composed of sp<sup>2</sup> hybridised carbon. As depicted in Figure 1, numbers of papers in indexed journals with the keyword

"coal carbon dots" has increased year by year since 2010. These data highlight the high research interest and potential of coal-based CDs. Therefore, the construction of CDs using coal and its derivatives is expected to become a key strategy to break the bottleneck of coal utilisation.

This paper will focus on the research progress of coalbased CQDs/GQDs. So far, many excellent review papers have been published on the synthesis, properties, and applications of coal-based CQDs/GQDs. 52-58 Among them, the fluorescence properties and synthesis methods of coal-based CODs/GODs have been well discussed, and the article will not go into details. However, a review on the formation mechanism of coal-based CQDs/GQDs has not been reported. In addition, functionalization of CDs is an effective way to adjust their surface state and intrinsic structure, and is also a current research hotspot. Therefore, the article briefly reviews the synthetic methods and physicochemical properties of CODs/GODs, focusing on the formation mechanism of coal-based CQDs/GQDs and their functionalization progress. Their applications in catalysis, bioimaging and chemical detection are discussed, as well as the exploration and prospects for future research. Hopefully, this paper will provide significant support for the design of efficient coalbased carbon nanomaterials and sustainable options for overcoming the bottleneck of coal applications.

# 2 Physicochemical properties of coal-based CQDs/GQDs

The structures and properties of coal-based CODs/GODs were analyzed using various characterization methods, such as XPS, SEM, TEM, FTIR, fluorescence and UV/Vis spectroscopy. Three basic characteristics were obtained by exploring their spectral features.

Investigation on the UV/Vis absorption spectra of coalbased CODs/GODs reported that the characteristic absorption peaks are usually attributed to  $\pi$ - $\pi$ \* leaps in the sp<sup>2</sup> structural domain and  $n-\pi^*$  leaps in some oxygen-containing functional groups. <sup>59–61</sup> Due to the  $\pi$ – $\pi^*$  leaps of the C=C bond in the sp<sup>2</sup> structural domain, coal-based CQDs/GQDs exhibit effective photon trapping ability in the short wavelength region. As a result, they typically exhibit strong light absorption in the UV region (260-320 nm) that extends into an end in the visible region.

The synthesis of coal-based CQDs/GQDs is usually accompanied by the introduction of a number of oxygenated and highly hydrophilic functional groups such as O-C=O, C-O and C=O, which further increase their solubility. 62-64 Therefore, solubility is also one of the most common

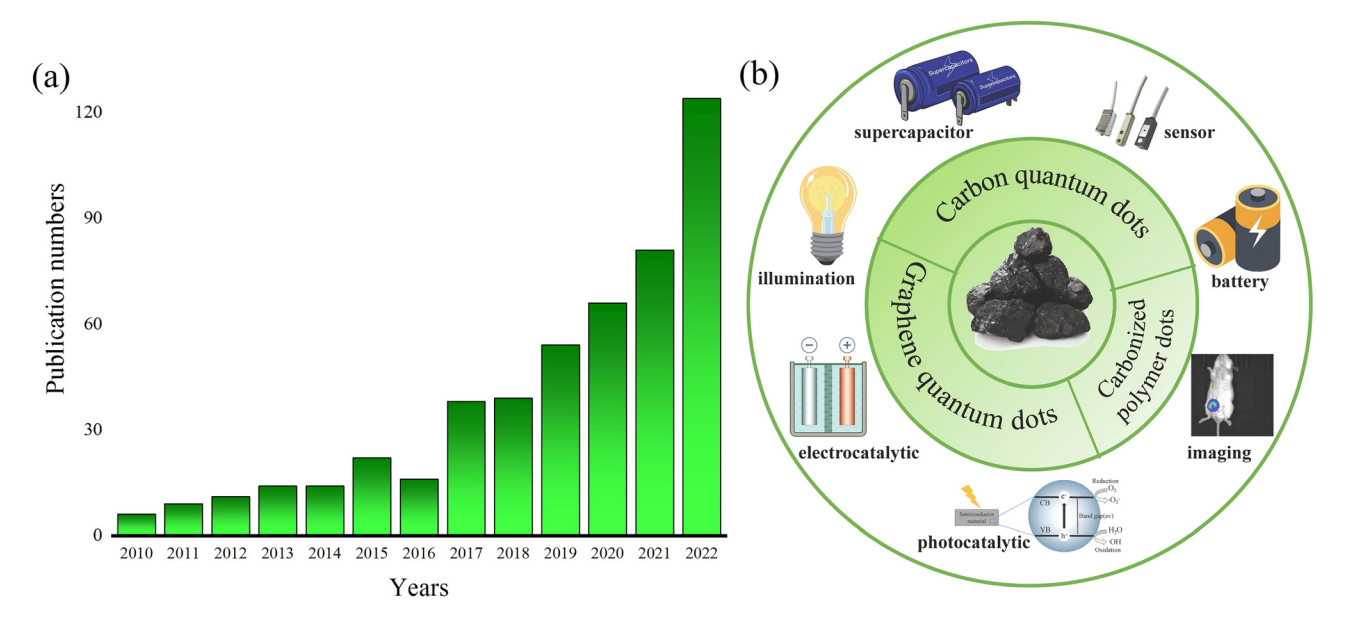


**Figure 1:** High research interest and application areas of coal-based CDs. (a) The number of publications with the Topic "coal carbon dots" from 2010 to 2023 obtained from ISI web of science; (b) coal-based carbon dots and their applications.

properties of coal-based CQDs/GQDs. Saikia et al. synthesized coal-based CQDs using ultrasound-assisted wet chemical method, and hydrothermal method, respectively. FTIR spectroscopy revealed that the surfaces of the CQDs synthesized by both methods possessed aromatic hydroxyl structures such as O–H, C–H, C–O and C=O. XPS analysis further confirmed all the synthesized CQDs contained sp² aromatic structural units and oxygenated groups such as carboxylic acid, hydroxyl and carbonyl. Thus, the CQDs exhibits high water solubility. However, not all coal-based CQDs/GQDs exhibit high solubility. CDs can be synthesised using direct microwave radiation using asphaltene as a carbon source. It was found that the prepared CDs possessed a small quantity of surface oxygenated functional groups and are highly carbonized by structural analysis, and exhibited a high degree of lipophilicity.

Fluorescence is one of the most attractive properties of coal-based CQDs/GQDs, in which the excitons generated by their absorption of photons rapidly recombine and release energy in the form of luminescence. Coal-based CQDs/GQDs differ from semiconductor quantum dots in that their fluorescence emission and light absorption do not originate from the bandgap and are usually closely related to their surface composition and intrinsic structure. Current studies suggest that the mechanism of the fluorescence properties is determined by quantum confinement effects or the surface states and defects of CQDs/GQDs. <sup>68,69</sup> Oxygenated groups (C–O, C=O, O–C=O) on the sp² sites of the aromatic ring, the partial conversion of the sp² hybridized C=C to the sp³ hybridized C–C, as well as the transformation of crystalline graphite to amorphous carbon lead to vacant lattice sites and defects

such as sp³ carbon. In addition, the fluorescence emission mechanism of coal-based CQDs/GQDs largely depends on the emission properties at the excitation wavelength. Carbon-containing solid particles quinoline insoluble (QI) can be used as a carbon source for the synthesis of highly fluorescent CDs. CQDs usually have size-dependent emission properties due to quantum confinement effects. T1-T3 The emission properties of the prepared CDs depend on their size and may also lead to variations in the nature and density of the available sp² sites in the CDs. CQDs can also be synthesised by chemical oxidation using coke as carbon source. Since the surface states can induce energy level structures, multiple energy levels in the different surface states of the CQDs exhibit excitation wavelength-dependent PL emission.

The excitation wavelength and structure of coal-based CQDs/GQDs can be adjusted by rationally changing the parameters such as ratio/composition of reagents and reaction temperature/time. Kundu et al. synthesized water-soluble coal-based GQDs using a wet chemical method and probed the stability of the GQDs.<sup>75</sup> The GQDs' PL intensity did not change significantly with irradiation time. Instead, the fluorescence properties of the GQDs was dependent on pH. The fluorescence intensity was maximum at pH 7, and the non-aggregated state showed a blue shift when pH changed to 13. This is attributed to the deprotonation of the carboxyl groups of the GQDs in alkaline solution which overcomes the tendency of aggregation of the layers stacked on top of each other. The red shift upon pH change to one is attributed to the aggregation in solution reducing the band gap. In addition, as the non-radiative decay rate increases with

increasing temperature, this leads to a subsequent decrease in the PL intensity of GQDs.

It is worth noting that when coal-based CQDs/GQDs are prepared using selective oxidation of H<sub>2</sub>O<sub>2</sub>, the PL intensity is usually affected by  $H_2O_2$ . The maximum emission peaks of the PL spectra of CODs shifted as the concentration of H<sub>2</sub>O<sub>2</sub> was varied. 76 CQDs excited at different wavelengths exhibited luminescence properties dependent on the emission and excitation wavelengths. Hu et al. also explored the effects of time, temperature and addition of H<sub>2</sub>O<sub>2</sub> to the reaction system on the PL intensity of the synthesized CDs. 68 It was found that the amount of OH was not linearly related to the amount of H<sub>2</sub>O<sub>2</sub> in the reaction system. The reaction temperature showed a nonlinear relationship with the PL -intensity, with the highest PL emission occurring at 80 °C. Too high a temperature promotes the decomposition of H<sub>2</sub>O<sub>2</sub> into O<sub>2</sub>, minimizing the production of ·OH. Too low a temperature inhibits the ability to convert H<sub>2</sub>O<sub>2</sub> to ·OH due to lack of energy. The amount of ·OH increases with reaction time thereby producing more product and therefore the PL intensity increases with reaction time. However, ·OH can attack the carbon atoms of crystalline nanoparticles containing epoxide and hydroxyl groups thereby depleting the formed CDs. Therefore, lower PL intensity is observed for too long reaction time.

Numbers of references focus on exploring and demonstrating the PL properties of coal-based CQDs/GQDs. Unfortunately, the exact origin of the fluorescence emission mechanism remains controversial due to their undefined chemical structures and surface moieties as well as inadequate characterization tools. Therefore, the relevant PL mechanisms need to be further explored.

# 3 Synthesis and formation mechanism of coal-based CQDs/GQDs

Coal can be classified as anthracite, bituminous, subbituminous, and lignite depending on the degree of coalification of the coal beds in time and depth.<sup>55</sup> In the last 80 years, more than 134 structural models for coals have been proposed.<sup>77</sup> Different classes of coals can be transformed into different products. Typically, lower-rank coals such as lignite and bituminous are low in carbon content and are rich in oxygen functional groups and low molecular compounds with random orientation. While high-rank coals such as anthracite have higher carbon and aromatic carbon contents and ordered molecular structures. The adoption of reasonable strategies for coals with different degrees of metamorphism is the key to realize the controllable synthesis of coal-based carbon materials.

Combined with the differences in carbonaceous precursors, the exploration of the formation mechanism of the prepared coal-based CQDs/GQDs is important to guide the synthesis of more efficient carbon materials. Unfortunately, the formation mechanism of the synthesized coal-based CQDs/GQDs is not clearly explained due to the unclear structure and the limitation of the characterization means. Therefore, some articles will resort to structural analysis to assist in understanding the formation mechanism.

## 3.1 Synthesis of coal-based CQDs/GQDs

Inrecent years, methods for synthesizing coal-based CQDs/ GQDs have emerged. Solvothermal and hydrothermal methods are the most common techniques, which have the advantages of low energy consumption, simple operation and no need for special reaction equipment. Notably, the oxidation process needs to be accomplished by tailoring the bulk coal and its derivatives with oxidizing agents. Commonly used oxidizing agents are H<sub>2</sub>SO<sub>4</sub>, HNO<sub>3</sub>, H<sub>2</sub>O<sub>2</sub> and O<sub>3</sub> etc. H<sub>2</sub>O<sub>2</sub> and ozone provide a milder oxidation process. However, due to the low product yields, there are fewer related studies. Oxidation of coal and its derivatives using strong oxidizing acids such as H<sub>2</sub>SO<sub>4</sub> and HNO<sub>3</sub> is currently the most common method. Notably, coal-based CQDs/GQDs prepared by this method usually introduce Nor S-containing groups. An orange fluorescent CQD with 605 nm long-wave emission has been synthesised in the literature by solvothermal method using coal tar as a raw material. 78 Analyzing the structure of the CQDs, it could be deduced that nitric acid oxidation introduces N-based groups including nitroxyls and O-based groups (e.g., hydroxyl groups).

Physical and electrochemical oxidation methods have also been used for the preparation of coal-based CQDs/GQDs, which are simple and time-consuming, but consume more energy. Among them, the electrochemical oxidation method can regulate the surface groups and particle size by solvent and applied current. However, the preparation of suitable coal-based electrodes requires a tedious pretreatment process.

Regardless of the synthesis method used to prepare coalbased CQDs/GQDs, they need to be purified by corresponding post-treatment processes to remove solvents and residues. Commonly used post-treatment processes are dialysis, centrifugation, filtration and rotary evaporation. The size of coal-based CQDs/GQDs may be affected by parameters such as dialysis time, centrifugation rate and membrane pore size. Thus, attention also needs to be paid to the purification of coal-based CQDs/GQDs.

Coal-based CQDs/GQDs synthesized by different preparation processes will have different microstructures, electron transfer capabilities, and photoluminescent properties. Ye et al. synthesized bandgap-tunable GODs using anthracite coal as a carbon source using two methods.<sup>79</sup> One is a onestep chemical synthesis method to prepare smaller-sized GQDs by successive warming, and the other is a chemical oxidation treatment and staggered flow ultrafiltration separation method. The band gap and size of GQDs synthesized by different methods are different. The photoluminescence of GQDs ranges from blue-green (2.90 eV) to orange-red (2.05 eV) due to differences in size, defects and functionality. Therefore, different methods can be used to customize the morphology of CQDs/GQDs, thus extending their applications in various fields.

Differences in the coal sources used as carbonaceous precursors can lead to differences in the products. Lowerorder coals may produce more oxygenated functional groups, while higher-order coals may provide more graphitized frameworks.<sup>55</sup> It was obtained that bituminous coals have smaller polyaromatic domains and more aliphatic chars, while coke and anthracite have a certain amount of graphite-like stacking domains, and the shapes and sizes of the prepared GQDs show significant differences.<sup>80</sup> In particular, the degree of coalization or coal rank does not determine the ease with which oxidative stripping of coalbased CQDs/GQDs occurs. Low-rank coals may be more prone to oxidative stripping to produce coal-based CQDs/ GQDs. One study used coal samples from six different coal systems as carbon sources to prepare single-layer GODs (S-GQDs).81 It was found that the yield of S-GQDs decreased with the increase of coal rank. Higher rank coals contain more carbon-based nanomaterials such as some CQDs, graphene oxide, and agglomerated carbon nanocrystals. Li et al. prepared symbiotic coal-based GQDs and coal-based graphene sheets (GS), and found that the GQDs and GS were distributed in different interlayers and were able to regenerate stably.<sup>82</sup> Moreover, the higher the reflectivity of the original coal, the larger the diameter of the GQDs, and the better the crystalline order of the symbiotic body.

## 3.2 Formation mechanism of coal-based CQDs/GQDs

## 3.2.1 Acid etching

Most of the current studies have utilized strongly oxidizing and corrosive acids such as H<sub>2</sub>SO<sub>4</sub> and HNO<sub>3</sub> to corrode

and oxidize coal and its derivatives. These acidic reagents in aqueous solution can disrupt the interlayer forces of coal and cut its large sp<sup>2</sup> carbon domains into small pieces. Combination of acidic oxidative etching and carbonization can fabricate coal into size-controlled fluorescent CDs. 83 Among them, the carbonization temperature is an important factor to control the size of CDs. The size of CDs is the smallest at 700 °C may be due to the gradual conversion of organic hydrocarbons in the coal to amorphous carbon at lower temperatures (400-700 °C), leading to the increase of amorphous carbon after acidic oxidation. As the carbonization temperature increases, the size of coal-based CDs increases. And these amorphous carbons may be transformed into crystals with fewer structural defects at higher temperatures (900–1500 °C). which makes the exfoliation of graphite crystals more difficult.

The two-step oxidation method also yields bandgaptunable CQDs.<sup>76</sup> First, pre-oxidation with K<sub>2</sub>FeO<sub>4</sub> as oxidants in H<sub>2</sub>SO<sub>4</sub> medium can form numerous active centers on the coal particles' surface. Subsequently, CQDs are obtained by oxidation with H<sub>2</sub>O<sub>2</sub>. Pretreatment with K<sub>2</sub>FeO<sub>4</sub>/H<sub>2</sub>SO<sub>4</sub> allows the sp<sup>3</sup> C–C bonds to be oxidized while the C=C bonds remain intact. 84 K<sub>2</sub>FeO<sub>4</sub> and H<sub>2</sub>SO<sub>4</sub> can be inserted into the interstitial spaces of coal molecules quickly. The oxidants react with water or H<sup>+</sup> to produce large amounts of oxygen while the aliphatic fraction is oxidized.85 As a result, non-covalent interactions such as hydrogen bonding,  $\pi$ – $\pi$  interactions, van der Waals interactions and electrostatic interactions are disrupted, leading to significant expansion of fly ash volume. In addition, oxidized coal has higher H<sub>2</sub>O<sub>2</sub> reactivity than raw coal. Therefore, controlling the concentration of H<sub>2</sub>O<sub>2</sub> can result in CODs with different bandgaps.

Direct coal liquefaction is a technology to convert coal into clean liquid fuels. The highly conjugated structure of coal is decomposed by catalytic hydrogenation in direct liquefaction into small aromatic structural. 86,87 However, direct liquefaction of coal produces a coal liquefaction residue that accounts to 30 wt% of the feed coal.<sup>88,89</sup> Qin et al. synthesized CDs using coal liquefaction residue as a carbon source and H<sub>2</sub>O<sub>2</sub>/H<sub>2</sub>SO<sub>4</sub> as an oxidizing agent and utilized a mild oxidation method. 90 H<sub>2</sub>O<sub>2</sub>/H<sub>2</sub>SO<sub>4</sub> solution selectively oxidized and cleaved the fatty chains obtained from liquefaction to obtain H<sub>2</sub>O and CO<sub>2</sub> and leaving behind stable conjugated fragments. As a result, CDs enriched in oxygen-containing functional groups such as-C=O and-COOH were formed at the edge sites. Unreacted coal liquefaction residue and ash were removed through centrifugation. This structure makes the prepared CDs more reactive and hydrophilic.

#### 3.2.2 Acid-free oxidative functionalization

In addition to the utilization of oxidizing acids, there are other oxidants such as H<sub>2</sub>O<sub>2</sub>, supercritical water or potassium persulfate that can also be used as oxidizing agents in the reaction system. These oxidizing agents cause oxidation or cleavage of coal fragments, which makes it easier to convert them into small-sized coal-based CQDs/GQDs. Coalbased GQDs can be synthesized by solvothermal method using potassium bisulfate as oxidizing agent. 91 This method does not involve acid oxidizing agents. The possible formation mechanism of GQDs involves a combination of free radical oxidation and solvent-thermal redox. First, potassium persulfate generates ·SO<sub>4</sub> or ·OH in a solvent thermal redox reaction. Graphite fragments of coal are reduced or cleaved by the resulting radical oxidation, providing an acidfree reaction for the synthesis of GQDs. Subsequently, coal is readily converted into very small-sized GQDs due to a combination of oxidative functionalization and solvent thermal cleavage. The synthesized GQDs are enriched with oxygenated functional groups such as hydroxyl, alkoxy, carboxylic acid and epoxy groups, that provide excellent dispersibility of GQDs in different solvents.

The molecular structure of coal tar pitch (CTP), which consists of an aromatic ring and several side chains attached to this ring, has a natural similarity to the structure of coalbased CQDs/GQDs. Compared with other materials, CTP is easier to be converted into coal-based CODs/GODs. The unique aromatic-core molecular structure of CTP leads to the crystalline nature of the prepared CQDs/GQDs. Shi et al.<sup>92</sup> and Liu et al. 93 synthesized homogeneously distributed CQDs and GQDs, respectively, by using CTP as a carbon source using a mild oxidation method with H<sub>2</sub>O<sub>2</sub>. The possible mechanisms for the formation of CQDs/GQDs from CTP are the same. That is, H<sub>2</sub>O<sub>2</sub> selectively oxidizes the edgeconnected alkyl chains of the CTP molecule to oxygencontaining groups. At the same time, the aromatic nuclei in the CTP molecule are retained and form the graphite domain structure of CQDs/GQDs.

CTP is an amphiphilic carbonaceous material that is soluble in alkaline aqueous solutions. Size-tunable CTPbased CDs can be obtained by hydrothermal method using NaOH as an additive. 94 The structural analysis suggests that the formation mechanism of CD is "bottom-up", i.e., dissolved nitro-pitch is converted into CD under the action of NaOH (Figure 2c). The minimum pH at which the asphalt dissolves is the threshold for this reaction, and after dissolution, it is functionalized by NaOH and part of the nitro group is converted to N\* (transition state). Subsequently, N\* binds to the aromatic ring and forms C-N-C, resulting in the formation of CDs. The hydrothermal reaction stops when the

pH is less than 12.15 with NaOH consumption. Thus, NaOH is very important in the dissolution of marginally functionalized and nitrified bitumen. Notably, the extent of the reaction increases with the consumption of NaOH and consequently the size of CDs increases.

Coal-based fluorescent CDs can be prepared by selective oxidation of H<sub>2</sub>O<sub>2</sub>.<sup>68</sup> The microstructure of coal exhibits organic carbon chains connecting crystalline domains, and the possible mechanisms for the formation of CD are shown (Figure 2a). It is commonly believed that the ·OH radical exhibits a strong oxidizing ability. When heated, the ·OH radical selectively oxidizes the organic carbon chains to H<sub>2</sub>O and CO<sub>2</sub>. While the stable crystalline carbon is retained thereby forming CDs. By exploring the process of OH formation using terephthalic acid (TA), it was verified that the thermal excitation energy can be effectively transferred to the hydroxyl groups of coal and the water absorbed on the surface thus producing ·OH (Figure 2b). A large number of COOH groups are found on the surface of CDs, which may be attributed to the decomposition of C=C and C-C bonds in coal by ·OH during the reaction process to produce more peripheral carbon to be produced by oxidation. 98 In addition, the O content of CDs was higher than that of coal proving the presence of ·OH-induced oxidative spalling occurring in coal. The possible formation mechanism of CDs was verified by analyzing the surface states and electronic structures of CDs.

Sasikala et al. prepared banded graphene materials with large aspect ratios using anthracite as a carbon source in a reducing environment provided by scEtOH, and monolayers of oxidized GQDs in high yields (55 wt%) in an oxidizing environment provided by scH<sub>2</sub>O.<sup>99</sup> Parallel pyrolysis and hydrolysis reactions have been reported to occur when heteroatoms containing groups in scH<sub>2</sub>O are linked to molecules containing saturated carbon.<sup>100</sup> First, the highly diffusive nature of supercritical fluids will result in the stripping of coal. Secondly, the shear effect generated by the high temperature and high pressure conditions of the reactor will combine with the disordered crystal structure and inherent heteroatom doping of the coal to cut large portions of its structure into fragments. The aspect ratio and size of the graphene material obtained through fracturing and exfoliation at this point are determined by the oxidizing nature of the supercritical fluid. In turn, the oxidation of scH<sub>2</sub>O is accompanied by a hydrothermal decomposition reaction that leads to the complete depolymerization of the coal, thus obtaining crystalline GQDs with smaller aspect ratios.

#### 3.2.3 Carbonization

Not all formation of coal-based CQDs/GQDs involves acid etching with oxidation. Carbonation can also induce the

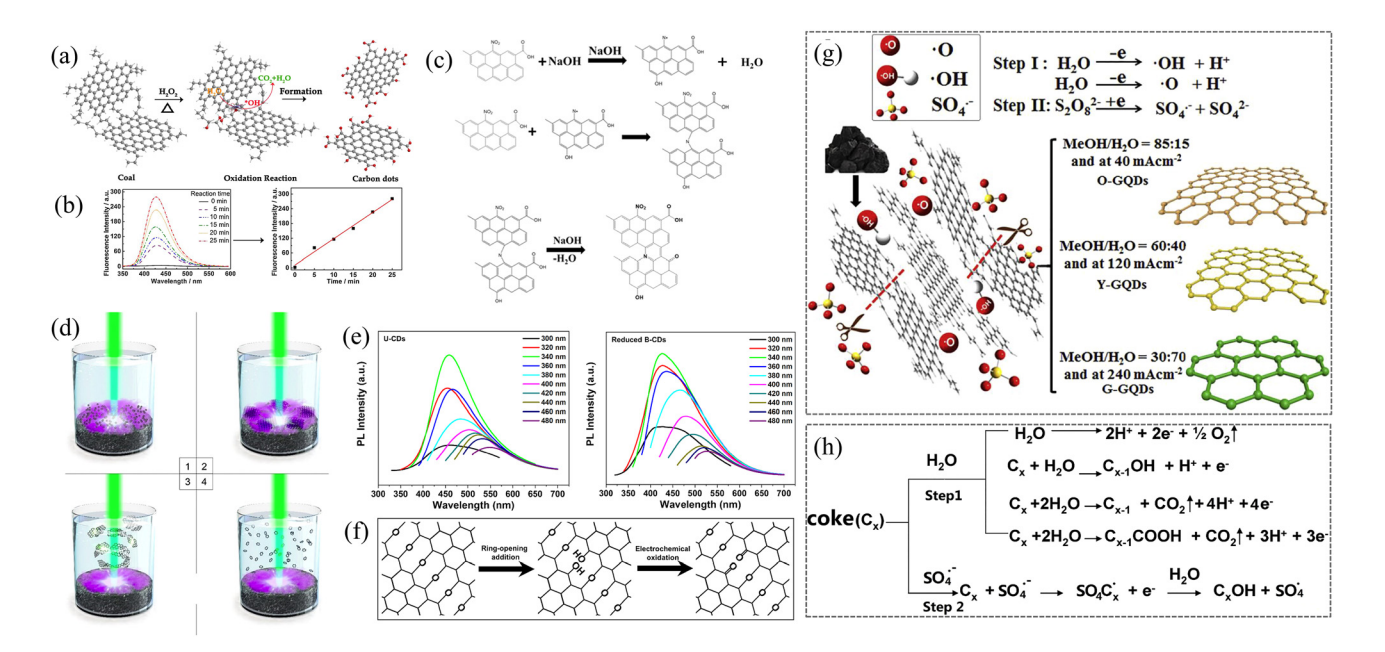


**Figure 2:** Mechanisms of formation of various types of coal-based CDs. (a–b) Formation mechanism of CDs in coal; <sup>68</sup> (c) Formation mechanism of CDs prepared from nitrified bitumen; <sup>94</sup> (d) Possible mechanism of coal conversion to GOQDs using PLAL method; <sup>95</sup> (e–f) Excitation PL spectra of relevant coal-based CDs when the excitation wavelength is varied in the range of 300–480 nm as well as the thermally-assisted electrochemical cleavage of graphite oxide into B-CDs by a possible mechanism; <sup>96</sup> (g–h) two-step formation mechanism for the synthesis of coal-based GQDs by electrochemical stripping. <sup>97</sup>

synthesis of CQDs/GQDs. Liquid coal biodegradation products (LPBCs) are produced during the biodegradation of coal. The LPBCs contain various oxygenated reactive functional groups such as quinone, phenolic hydroxyl, and carboxyl groups, as well as low relative molecular masses. LPBC can be used as a carbon source to synthesise CD using hydrothermal methods. During the synthesis process, organic small molecules in LPBC gradually formed sp<sup>2</sup> and sp<sup>3</sup> hybridized carbon nuclei through polymerization and carbonization. The carbon core extends to the surface of the nanoparticles through other molecules and then continues to grow to obtain the blue-green fluorescent CD. Unfortunately, the formation mechanism of CD is not yet completely clear, and further exploration is needed.

### 3.2.4 Physical bond breaking

When coal is treated using physical processes such as laser or ultrasound, the high energy breaks the bridge bonds in the coal, which results in the fragmentation of the coal into small nanoparticles. Typically, the reaction also requires the addition of a solvent in order to facilitate the dispersion of small particles. Coal-based CDs can be prepared by pulsed laser ablation using ethylenediamine (EDA) as surface passivator and reaction solvent. The pressure and temperature at the reaction sites during pulsed laser ablation were very high, so that the cleavage of ether,

alkene, and methylene bonds along the thermally unstable ester bonds was more likely to occur. Temperature-activated chemical reactions carried out by EDA accompany the breaking of these bonds and promote their effective surface passivation. It is shown that the quantum confinement effect is effective in modulating the wavelength-dependent emission behavior only when the CDs are very small in size.

Coal-based GQDs (C-GQDs) can be prepared by one-step ultrasonic physical shear method. 103 Ultrasonic irradiation action breaks down the bridging bonds in the coal, resulting in nanoscale sp<sup>2</sup> carbon crystal structures with many edge defects. The prepared C-GQDs exhibited two different fluorescence emission patterns. Electronic structure analysis and the evolution of surface states indicate that the longwavelength emission and short-wavelength emission are mainly attributed to the  $n-\pi^*$  leaps of oxygen-containing groups as well as the  $\pi$ - $\pi$ \* leaps of sp<sup>2</sup> conjugated carbons. CDs can be synthesized from low-grade, high-sulfur coals using wet-chemical ultrasonic stimulation induction.<sup>104</sup> Low-grade coals have been reported to typically have graphite-like polyaromatic structures. 43 Therefore, the graphitized and non-graphitized polycyclic aromatic hydrocarbons (PAHs) present in the coal were exfoliated during ultrasonic treatment of high-sulfur coal in the presence of H<sub>2</sub>O<sub>2</sub>. The PAHs fragments were further decomposed into C2 carbon units, which formed CDs through polymorphic

reactions. In addition, hydrogen in raw coal is important in the formation of CDs. 105-107

Pulsed laser ablation liquid (PLAL) technique can be used to synthesize coal-based graphene oxide quantum dots (GOODs). 95 The possible formation mechanism of GOODs from coal is shown (Figure 2d). Solid target surfaces undergo Coulomb explosion during laser pulse injection. The plasma plume first forms around the target coal, which is attributed to the absorption ionization of multiphotons. 108 Subsequently its expansion and cooling occur leading to the creation of cavitation bubbles in solution. When the temperature and pressure inside the bubble are lower than the surrounding solution, the carbon clusters in the cavitation bubble are ablated away from the target while still having a high surface energy, which tends to aggregate and form layered graphene sheets. The graphene sheets are further ablated by the injected laser to form nanoscale GOODs. It is notably important to note that the use of a laser source with a low power density will affect the formation of GOQDs. Different cooling rates within the plasma plume may also affect the size of GOODs.

### 3.2.5 Electrochemical stripping

Electrochemical flaking has the advantages of high yield, high efficiency, low cost and easy operation. The mechanism of electrochemical oxidation is usually divided into two: one is the intercalation of anions; the other is the attack of free radicals, which act like "scissors" to break the connection between graphite domains. The surface functional groups and particle size of coal-based CQDs/GQDs can be realized by controlling the concentration and type of electrolyte on the electrode and the current density.

Multicolor fluorescent GODs could be obtained by applying current density and adjusting the aqueous solution of electrolyte using coke as a carbon source.<sup>97</sup> The possible mechanism of formation of GQDs can be divided into two key steps (Figure 2g). The H<sub>2</sub>O plays a very important role in step one. It has been reported that ·O and ·OH radicals generated from the decomposition of H<sub>2</sub>O can exfoliate coke into multilayer graphene sheets by efficient electrochemical oxidative cleavage. 109,110 Firstly, the free radicals attack the edge surface of coke to accelerate its oxidation or hydroxylation process, thus promoting the formation of more edge flakes on the edge surface. 111 (NH<sub>4</sub>)<sub>2</sub>S<sub>2</sub>O<sub>8</sub> as a specific electrolyte plays a very important role in step II.  $SO_4$  radicals with strong oxidizing properties are formed through the electrochemical reaction of  $S_2O_8^{2-}$ . The opening of the edge sheet allows the successful insertion of the SO<sub>4</sub> radicals into the lamella. Subsequently, the product obtained from the splitting of the lamella by the radical expands in the stacking direction, favoring the destruction of the weaker aliphatic C-C bonds. The stronger aromatic C-C bonds, on the other hand, will mostly remain intact and integrate to form aromatic crystalline carbon structures thereby forming nanoscale GODs. 112 The electrochemical reaction mechanism involves complex interactions between O, OH and SO<sub>4</sub> radicals (Figure 2h). Notably, the concentration of ·O and ·OH radicals in the electrolyte solution increases with increasing H<sub>2</sub>O, thereby cutting the coke into smaller graphene flakes. The SO<sub>4</sub> radicals further exfoliate these graphene flakes into GODs with a fluorescence-emitting blueshift. Conversely, the amount of GQDs with a fluorescenceemitting redshift will increase with decreasing H<sub>2</sub>O content.

Coal-based bimodal emission carbon dots (B-CDs) can be synthesized using thermally assisted electrochemistry. 96 The B-CDs exhibited PL emission under single-wavelength excitation at 510 and 415 nm, respectively (Figure 2e). This is attributed to the coexistence of carbonyl-associated surfacestate PL centers and core-state PL centers generated on the B-CDs surface under thermal induction. The possible formation mechanism is shown (Figure 2f). First, oxidizing conditions oxygen atoms bind to the graphite surface and form two-legged epoxy bridges. In order to reduce the energy, they align and create a collective tension breaking the underlying C-C bond. 113,114 Subsequently, the hydroxyl groups in the basic electrolyte undergo a thermally assisted ring-opening addition reaction with the epoxy groups and form hydroxyl pairs attached to the edge carbon atoms. During electrochemical oxidation, the hydroxyl pairs are further converted to carbonyl pairs. Then, the flaky B-CD was separated from the bulk graphite. The prepared B-CDs had carbonyl groups immobilized on the surface/edge and contained relatively large sp<sup>2</sup> (graphene-like) structural cores.

# 4 Functionalization of coal-based CQDs/GQDs

Coal-based CQDs/GQDs show great potential for applications in many fields owing to their excellent physicochemical properties. In order to further improve their photophysical and photochemical properties and extend their applications, the functionalization of coal-based CQDs/GQDs has been proposed. Currently, the three main functionalization strategies are surface modification, material hybridization and heteroatom doping. It has been shown that surface functionalization can modulate the internal electronic structure and provide abundant active sites, thus enhancing the selectivity of coal-based CQDs/GQDs and applying them to

different fields. 115,116 Surface modification of the surface functional groups of coal-based CQDs/GQDs allows them to retain the unique properties possessed by functional ligands. Whereas, heteroatom doping is mainly used to adjust their intrinsic properties.

### 4.1 Surface modification

Surface modification is a strategy to functionalize coal-based CODs/GODs with functional ligands, such as polymers or organic molecules, by chemical bonding or physical mixing, which can increase the number of active sites and change their surface state.

The preparation of double peaked carbon dots (D-CD) can be realized by using coal-based CD as the crystalline material and diammonium phosphate (DAP) as the modifier. 117 The thermotropic surface modification of coal-based CD by DAP and reaction temperature was the main reason for the formation of D-CD. Structural analysis indicated that P-containing and N-containing groups were introduced into the CD through DAP functionalization, which was the source of the double PL peak emission. The possible formation mechanism of the PL of D-CD is shown (Figure 3a and b). As previously reported, O-containing groups on sp<sup>2</sup> hybridized

carbons can induce significant local distortions and subsequently generate different energy levels (called O states) below their lowest unoccupied molecular orbitals (LUMOs). 118 The O states produce excitation-dependent PL emission as the excitation wavelength increases. The amine group introduces a new energy level below the LUMO (called N state). The energy level decreases with increasing number of NH<sub>2</sub> groups. The N state acts as an electron trapping platform at specific energy levels, which facilitates efficient radiative complexation. When the excitation energy is higher than the excitation energy of the N state, the R1 emission of D-CDs dominates and exhibits excitationindependent emission properties. And the excellent electron-donating ability of the P-containing groups promotes the energy level states (called the P state) above the highest occupied molecular orbital (HOMO). The R<sup>2</sup> emission caused by the jump between the P state and the N state occurs at the same time as that of the R1, resulting in the D-CDs exhibiting bimodal PL emission.

Surface modification of coal-based CQDs can be achieved by grafting organic amino molecules. 122 The CODs modified by different organic modifiers exhibit similar PL emission spectral properties with only slight displacement of the emission peaks. The amine-grafted CQDs exhibited enhanced PL intensity to varying degrees. Notably, the

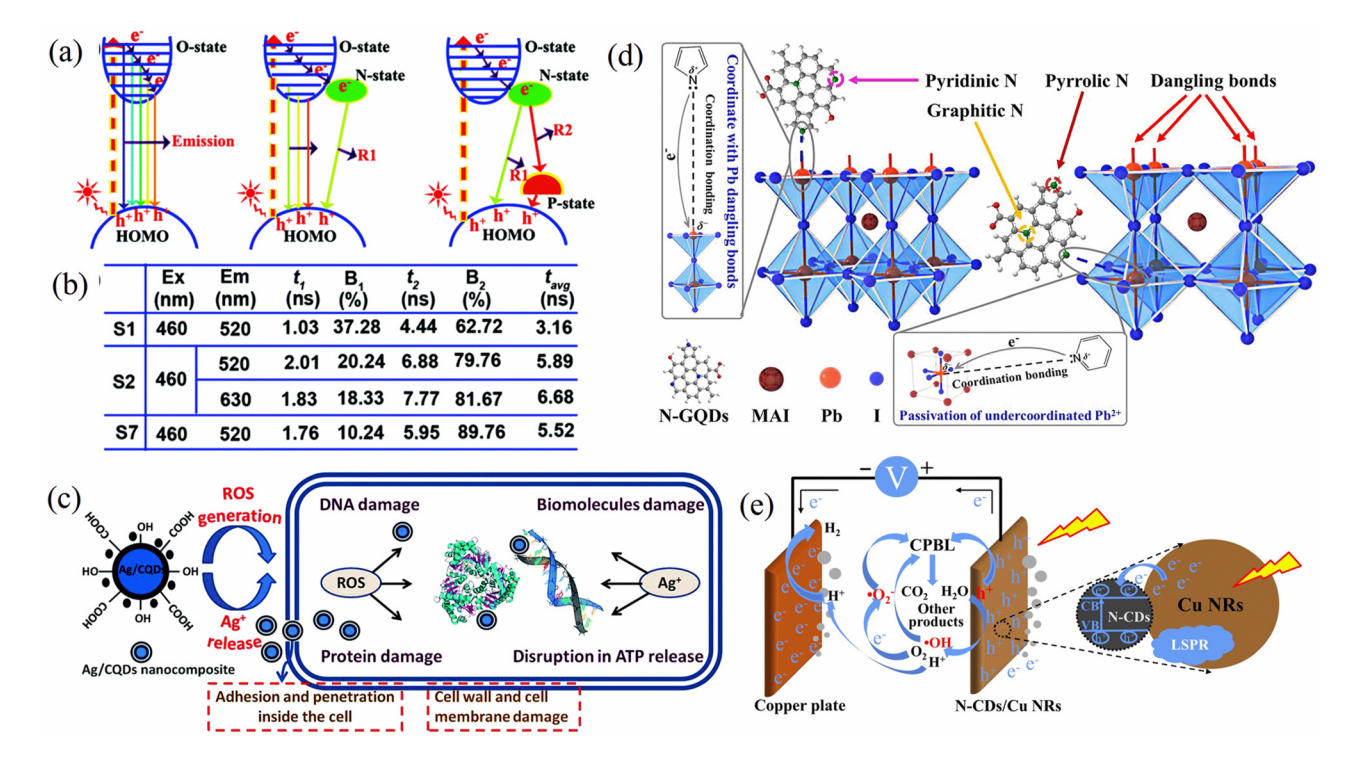


Figure 3: Mechanisms of action of various types of coal-based CDs. (a-b) schematic representation of PL mechanism of coal-based D-CD. 117 (c) Schematic representation of possible mechanism of action of Ag/CQD nanocomposites. 119 (d) Schematic representation of the passivation mechanism of N-GQDs of MAPbI<sub>3</sub> chalcogenides.<sup>120</sup> (e) Study on the degradation of CPBL and hydrogen production mechanism by PEC.<sup>12</sup>

EDA-grafted CQDs had the highest quantum yield. This may be attributed to the specific proton transfer from the amine ligand to the conjugated fluorophore-like structure. Nilewski et al. reported the polyethylene glycol (PEG) functionalization of coal-based GQDs. 123 Quinone and carboxyl groups are the main oxygenated functional groups in GODs, which have fewer C-O bonds as well as increased carboxylic acid groups. In contrast, the PEGylated GQD samples exhibited an increase in C-O bonds and a decrease in free carboxylic acids as they were converted to amides.

## 4.2 Material hybridization

To further extend the functionality of coal-based CODs/ GQDs, combining them with other materials to form heterogeneous materials is also an effective strategy. The nanomaterials used to construct the composites are mainly metals and oxides, etc. TiO<sub>2</sub>, FeS, and  $\alpha$ -Fe<sub>2</sub>O<sub>3</sub> have been used to composite with coal-based CQDs/GQDs to form heterostructures and applied in the field of catalysis. The construction methods mainly include in situ growth, chemical bonding and physical mixing. The construction of novel coalbased CODs/GODs composites is of great significance to broaden their applications. In particular, Ag as a noble metal particle has received increasing attention owing to its stability and surface plasmon resonance (SPR) effect.

Ag/CDs composites were obtained by in situ attachment of synthesized coal-based CDs to Ag surface using silver mirror reaction. 124 CDs contain reducing groups such as CN and CHO on their surface. Under the action of the reducing agent PEG-400 and heating and stirring, the reducing groups were oxidized to oxygen-containing groups such as COOH, and the complex ion [Ag(NH<sub>3</sub>)<sub>2</sub>] OH in the silver NH<sub>3</sub>·H<sub>2</sub>O solution was reduced to Ag nano-particles (NPs). The CDs containing numerous groups such as COOH, CN, and CHO formed Ag-O bonds or chelated adsorbed on the newly formed Ag particles, thus inhibiting the further growth of Ag nanoparticles. Ag/CQD nanocomposites can also be obtained using coal-based CQD as stabilizer and reducing agent (Figure 3c). 119 Silver exists in Ag/CQD in the oxidation state of metal zero-valent. Usually, the ability of metal particles to attach to the surface of carbon nanostructures is attributed to the existence of oxygenated functional groups such as phenolic, carbonyl, and carboxyl groups on their surfaces. Another hypothesis is that metal particles are also attractive to carbon nanostructures that lack oxygen-containing functional groups. 125,126 So the interaction of oxygen with functional groups on CQDs with AgNPs and the correlation between the d orbitals of Ag and the  $p/\pi$  orbitals of carbon in AgNPs are considered to be responsible for the generation of

Ag/CQDs. It was observed by surface state and electronic structure analyses that CQDs are functionalized by oxygenated functional groups and are surface-associated with functional groups with negative surface charges. The cationic Ag<sup>+</sup> ions readily coordinate with the functional groups on the COD surface and reduce themselves to Ag (0). As a result, AgNP is generated on the surface of CQD and does not aggregate with the help of surrounding edge charges.

## 4.3 Heteroatom doping

Heteroatom doping is a common surface functionalization strategy. Some elements such as N, P, S, and B have been used as dopants to replace carbon atoms in the sp<sup>2</sup>/sp<sup>3</sup> network. Typically, heteroatom-doped coal-based CQDs/GQDs can be synthesized directly by direct carbon-activated heteroatomrich carbonaceous materials or by in situ doping. Heteroatom doping can effectively modulate their electronic distributions and structures, including metal doping and nonmetal doping.

Among various nonmetals, N doping is a very important means. C and N have similar atomic radii and are adjacent to each other in the periodic table. Therefore, N doping in coalbased CQDs/GQDs is a powerful means to improve their material properties and adjust their material structures. The prepared coal-based CQDs/GQDs usually have nitrogencontaining functional groups such as-NO2 and amino groups, as well as oxygenated functional groups such as hydroxyl and carboxyl groups, thus achieving successful N doping and surface functionalization of CDs, which exhibit good hydrophilicity. 127,128 Li et al. prepared coal-based N-CDs using anthracite as a carbon source in the presence of dimethylformamide. 129 The sp<sup>2</sup> carbon structural domains in anthracite and the neighboring layers were connected by bridge bonds to form its macromolecular structure. Firstly, the light component in anthracite can be well dispersed into the solvent during solvent heating. At the same time, the partially decomposed dimethylamine from dimethylformamide can be doped into the sp<sup>2</sup> carbon structural domains by nucleophilic ring-opening reaction with bridge bonds between adjacent layers. As a result, smaller-sized sp<sup>2</sup> carbon structures in anthracite are stripped out and form N-CD. Compared with the acid oxidation method, the N-CD prepared by this method has more conjugated structures and fewer functional groups.

Hu et al. prepared coal-based N-GQDs by chemical reagent oxidation (Figure 3d). 120 The main forms of doped N are pyridine nitrogen and pyrrole nitrogen, and graphitic nitrogen has the lowest content. And the electron-rich pyridine nitrogen in N-GQDs can be used as Lewis bases with

uncoordinated lead ions to form coordination bonds through shared electron pairs, thus decreasing the defect density and nonradiative complexation of photogenerated electron holes and prolonging the carrier lifetime.

Loading coal-based N-CDs onto Cu nanorods, composite catalysts N-CD/Cu NRs can be obtained by ammonia thermal cutting method (Figure 3e). 121 Structural analysis showed that coal-based N-CDs exhibit good hydrophilicity because their main components are aromatic structures linked to oxygen- and nitrogen-containing groups such as amino, carboxyl, hydroxyl and epoxy groups. The C-O peak of N-CD/Cu NRs disappeared after hydrothermal synthesis compared to coal-based N-CDs. This is probably attributed to the formation of -CONH- (amide bond) by the C-O functional group on the N-CD surface during hydrothermal synthesis. N-CD/G hybrids can be obtained by combining coal-based N-CD with GO by hydrothermal method. 130 Graphene was used as a carrier for immobilizing and dispersing N-CD to avoid CD aggregation and to facilitate fast electron transfer effects. Structural analysis shows that N-CD is uniformly dispersed on the surface of graphene and plays an important role as a catalytic site. And N-CD/G contains oxygen-containing functional groups such as C-O, C=O and O-C=O. The presence of these functional groups makes N-CD more hydrophilic under alkaline conditions, resulting in a stronger affinity for electrolytes and dissolved oxygen.

N and B are a novel pair of double dopants. Fei et al. synthesized coal-based GQDs and self-assembled them on graphene to form nanosheets, followed by high-temperature annealing to form N- and B- co-doped carbon nanomaterials (BN-GQD/G). 131 The high specific surface area of GO acted as a two-dimensional template guiding the assembly of GODs. Strong interactions between the carbonyl and hydroxyl functional groups of GODs and GO ensured a tight stacking between them and the formation of GQD/G hybridized nanosheets. In particular, when GQD is in excess, the surface area provided by GO is not sufficient to support GQD and thus severe aggregation occurs. The abundant oxygencontaining functional groups and exposed edges of GQD facilitate the doping of dopants. The doping amounts of B and N can be adjusted by varying the doping time. When the doping amount is increased, B and N tend to exist in pairs.

Co-doping of GQDs with heteroatoms such as S, P, and N has been determined to be an effective way to enhance QY by introducing defects and adding more coordination sites. 132–135 Due to the synergistic coupling effect between the heteroatoms, co-doping can produce more catalytically active centers than monoatomic doping. S, P, and N co-doped coal-based GQDs (NPS-GQDs) were synthesized by a one-step wet chemical and dialysis method. 136 The localized doping of S, P, and N on GODs can reach the levels of 3.7 %, 3.7 %, and

5.6 %, respectively (on an atomic basis). S, P and N introduced more defects and disorder at the edges and bottoms of coal-based GQDs. The prepared NPS-GQDs surface contained numerous hydroxyl and amino groups and showed good hydrophilicity. In order to investigate the formation mechanism of NPS-GQDs, four types of coal with different coal rank, namely, coal ash, anthracite, coking coal and lignite, were synthesized as carbon sources. The basic units of the coals are connected to each other by bridge bonds such as -S-, -O-, -CH<sub>2</sub>-O- and-CH<sub>2</sub>-CH<sub>2</sub>-. Their edges are usually capped with alkyl side chains and other functional groups. The higher the coal rank or the higher the degree of coalification, the fewer the functional groups and side chains. During the formation of GODs in coal, an oxidant is inserted into the coal and oxidizes the interlayers of the graphitic structure in the coal. Layer spacing increases with the degree of oxidant penetration, and bridge bonds break at weak points and form GQDs. Typically, the number of benzene rings in the coal basic unit is referred to as the degree of graphitization. Raw coals with either too low or too high a degree of graphitization are not successful in synthesizing high-quality GQDs. Thus, coals with the right degree of graphitization are largely capable of forming homogeneous, short-range-ordered, but long-range-disordered GQDs.

Metal doping can also improve the physicochemical properties of coal-based CQDs/GQDs. Lanthanide fluorescent complexes have been widely used as fluorescent probes in various fields. Among them, Eu(III) complexes have great advantages due to their long PL lifetime, large Stokes shift and their narrow emission at long wavelengths. Trinchet et al. prepared Eu(III)-doped surface-modified CQDs with hydrophobic coatings.<sup>137</sup> This surface functionalization not only changes the accessibility of water molecules to Eu, but also improves the dispersion of the nanoparticles in nonpolar media.

Surface modification, material hybridization and heteroatom doping are all functionalization strategies that can effectively tune the intrinsic structure of coal-based CQDs/GQDs and change their physicochemical properties. Unfortunately, it is still difficult to explain how functionalization changes the intrinsic structure, which deserves further investigation in the future.

## 5 Application

## 5.1 Sensing

Coal-based CQDs/GQDs have been widely used in different fields due to their excellent physicochemical properties. Among them, the use in the sensing field is the more

frequent report that appeared. Sensors based on coal-based CQDs/GQDs exhibit high selectivity and low detection limits. The remarkable fluorescence properties exhibited by coalbased CODs/GODs can be used as probes for ion detection in bioanalysis and environmental protection. The mechanism of luminescent sensors is primarily founded on bursting or restoring the fluorescence emission of coal-based CQDs/ GODs in the presence of analytes. 138,139 Currently, the analytes have been extended from common heavy metal ions to inorganic molecules and biomolecules. In addition, coalbased CODs/GODs have been applied in temperature and PH sensing devices because they exhibit some sensitivity to temperature and PH. Generally, the fluorescence on/off method is the main design method for sensor systems.

#### 5.1.1 Detection of metal ions

Toxic heavy metal ions such as lead, silver, copper, cadmium and chromium (VI) are widely used in a large number of food, pharmaceutical and agricultural plants. The release and accumulation of these ions occurs thus jeopardizing the ecosystem and human health. Detecting the concentration of metal ions in the environment is of great significance for the safety of the food chain and human health. Previous detection methods include atomic absorption spectroscopy (AAS) or ionization mass spectrometry (IMS). Recent studies have begun to use CODs to detect metal ions in a simple and economical way. Das et al. investigated the fluorescence emission properties of coal-based CDs in buffer solutions containing different metal ions.<sup>104</sup> The results showed that Ag<sup>+</sup> exhibited the highest tendency to fluorescence burst. Surface charge analysis showed that the cation Ag<sup>+</sup> has a tendency to coordinate with the functionalized CDs. The surface oxygen-containing functional groups of CDs reduce Ag<sup>+</sup> to Ag<sup>0</sup> thereby forming Ag nanoparticles. Whereas, silver nanoparticles get stabilized without aggregation with the help of external charge of CD. Hu et al.<sup>83</sup> and Zhang et al.<sup>103</sup> used the prepared coal-based CDs and coal-derived GQDs (C-GQDs) as fluorescent probes to detect various metal ions present in water, respectively. The results showed that Cu<sup>2+</sup> exhibited the highest selectivity for both prepared coalbased CDs with significant bursting effect. The former may be attributed to the rapid metal-ligand binding kinetics and high thermodynamic affinity of Cu<sup>2+</sup> for N,O-chelating groups on the surface of coal-based CD, with a detection limit as low as 2.0 nM. Thus, Cu<sup>2+</sup> quenches the fluorescence of CD in the presence of an electron or energy transfer. The latter is attributed to the multisite coordination of oxygencontaining groups with Cu<sup>2+</sup> in C-GQD. In the range of  $0-8 \mu mol L^{-1}$ , the  $Cu^{2+}$  concentration showed a linear

relationship with the C-GQD fluorescence intensity ratio of the burst (Figure 3a and b).

Coal-based N-CODs can detect both Cu<sup>2+</sup> and Fe<sup>3+</sup>. 127 The PL intensity of the N-CODs solution decreased gradually with increasing Cu<sup>2+</sup> and Fe<sup>3+</sup> concentrations in the range of  $0-50 \mu M$  (Figure 3c-f). This may be due to the fact that  $Cu^{2+}$ and Fe<sup>3+</sup> with N-CQD can form non-luminous ground state complexes. The electrons of the complexes return to the ground state under UV irradiation without any photon emission, and thus fluorescence burst occurs. The detection limits of the sensor for Fe<sup>3+</sup> and Cu<sup>2+</sup> were 0.1731 M and 0.161 M, respectively. Particularly, owing to the redox reaction of Fe<sup>3+</sup> with L-ascorbic acid, Fe<sup>3+</sup> is detached from the surface of the N-COD upon addition of L-ascorbic acid, thereby restoring the fluorescence of the N-COD. Thus, the amount of L-ascorbic acid can be measured by using a sensing system comprising N-CQD and Fe<sup>3+</sup>. Chu et al. used the synthesized CD as a fluorescent probe for the detection of Eu<sup>3+</sup>, Tb<sup>3+</sup> and Fe<sup>3+</sup> with detection limits of 0.79, 0.10 and 0.019 μM, respectively.<sup>62</sup> Fe<sup>3+</sup> exhibits strong coordination with the phenolic hydroxyl group at the edge of CD and there is a fast electron transfer process between them. The excited state electrons of CD are transferred to the unfilled orbitals of the ligand Fe<sup>3+</sup> to trigger non-radiative electron/hole complexes, and thus the fluorescence of CD is burst (Figure 3g and h). The liganding ability of CD under strong adsorption promotes the formation of stable CD-Tb/Eu complexes. The lowest excited state energy levels of Eu<sup>3+</sup> and Tb<sup>3+</sup> ions match the triplet state energy levels of CD. Therefore, the excited CD can transfer its adsorbed energy to the Tb<sup>3+</sup> and Eu<sup>3+</sup> ions via nonradiative leaps, enhancing the luminescence of their ions themselves.

Pb<sup>2+</sup> had a significant bursting effect on the fluorescence of NPS-GQDs. 136 The reason for this is that that the sulfhydryl and hydroxyl groups of NPS-GQDs have fast chelation kinetics and strong binding affinity with Pb2+, which alter the exciton distribution and electronic structure of NPS-GQDs. The addition of Pb promotes nonradiative complexation of excitons through an efficient electron transfer process within the GQDs (Figure 3i-k). The excited state electrons are transferred from the NPS-GQD to the LUMO of the Pb<sup>2+</sup> cation. And the electrons return to the ground state of the NPS-GOD by radiationless transfer, which leads to its fluorescence burst. Notably, Fe<sup>3+</sup> can interfere with Pb<sup>2+</sup> due to its bursting effect on NPS-GQD. However, the Fe<sup>3+</sup> concentration did not show a linear relationship with the fluorescence intensity of the burst. Ascorbic acid can act as an effective reducing agent to eliminate the interference of Fe<sup>3+</sup>. Therefore, NPS-GQD can be used as a fluorescent probe for the detection of Pb<sup>2+</sup> with an absolute detection limit of  $0.75 \mu M$  in the 1–20  $\mu M$  range.

Particularly, the fluorescence of coal-based CQDs/GQDs can undergo recovery in the presence of GSH, and thus they can be used as a tool for the detection of GSH. Zhang et al. prepared two solid sensors using coal-based N-CDs with polyacrylamide network and filter paper. 128 The NCDs were doped into the NCDs-PAM hydrogel constructed by polyacrylamide network or the paper-based sensor constructed by adsorbing NCDs onto the fiber structure of filter paper was sequentially immersed in Hg<sup>2+</sup> and GSH solutions. It was found that the fluorescence was quenched by  $Hg^{2+}$  ions and recovered in GSH solution.

Coal-based GODs can be used to detect GSH and Mn ions (7<sup>+</sup> and 2<sup>+</sup>).<sup>75</sup> The fluorescence of GQDs was burst in the presence of Mn<sup>n+</sup>. Interestingly, the GODs showed remarkable variations in fluorescence intensity and steady-state absorption. However, the excited state lifetime values remained constant in the existence of different Mn<sup>n+</sup> bursting agents. Thus, the GODs are realized by a static bursting mechanism with Mn<sup>n+</sup>. Moreover, the fluorescence of GQDs was restored in the existence of GSH. Therefore, the GODs-Mn<sup>n+</sup> nanoprobe system can be efficiently applied to the selective and sensitive analysis of GSH through the fluorescence "off-on" mechanism. The detection limits of A-GQDs-Mn<sup>7+</sup>, BGQDs-Mn<sup>7+</sup>, B-GQDs-Mn<sup>2+</sup> and A-GQDs-Mn<sup>2+</sup> were 36 mM, 27 mM, 99 mM and 96 mM, respectively in the presence of GSH.

#### 5.1.2 Detection of compounds

It has been shown that coal-based CQDs exhibit high selectivity and high sensitivity for phenol detection.<sup>63</sup> The carboxyl groups on the CODs surface can form hydrogen bonds with phenol and promote fluorescence bursting of excited-state fluorescent CQDs with detection limits as low as 0.076 mM. Liu et al. constructed a 2,4,6-trinitrophenol (TNP) fluorescent sensor by loading prepared asphaltene-based CD into polymer micelles.<sup>67</sup> The nonionic triblock copolymer formed micelles with hydrophilic surfaces and hydrophobic inner cavities. The CDs was protected by the micelles to enhance the emission by 2.89-fold. This is attributed to the fact that the spectral overlap that exists between the emission of CD and the absorption of TNP permits the transfer of energy from the excited state of CD to the ground state of TNP, which leads to fluorescence quenching of CD. 140 Furthermore, it was found that compounds other than TNP also exhibit a small amount of fluorescence burst by comparing different aromatic nitro compounds with similar structures. This is attributed to the presence of nitro group which makes these compounds exhibit strong electrondeficient properties, whereby electron transfer from CD to the receptor of aromatic nitro compounds occurs. 141 Thus,

TNP significantly bursts the fluorescence through an electron transfer and energy transfer mechanism, resulting in a high sensitivity of CD to TNP.

#### 5.1.3 Detection of temperature and pH

Hu et al. 117 and Ran et al. 96 prepared coal-based CDs with dual PL peaks all showed significant pH-sensitive behavior. In the former study, the intensities of the two PL peaks of D-CD showed fluorescent colors with distinguishable differences with pH. The ratio of the PL intensity of the two emission peaks decreased with increasing pH and showed good linear correlation with pH over a wide range by the correlation equation. Moreover, the dual emission peaks of D-CD were almost unaffected by metal ions. In the latter study, the intensity ratio of the dual fluorescence peak (I415 nm/I510 nm) increased linearly and rapidly in the pH range of 10.6-13.4. Therefore, B-CDs can be used as ratiometric fluorescent nanoprobes in this pH range. The results indicate that the two coal-based CDs have strong pH dependence and are suitable for application in pH sensing. Zhang et al. synthesized CDs with LPBC as the carbon source with temperature and pH sensitivity, and their fluorescence intensities showed good linearity in the temperature range of 30-65 °C and pH 3-8, respectively. 101 The refilling or depletion of VB on CDs upon pH change can lead to changes in the electron leaps of  $n-p^*$  and  $p-p^*$  in graphite nanodomains. Meanwhile, protonation and deprotonation of amino, hydroxyl, and carboxyl groups on CD can induce its Fermi energy level shift to produce pH-dependent luminescence. When the temperature increases, more nonradiative channels of CD are activated and aggregated, resulting in fluorescence burst and temperature-dependent luminescence.142, 143

#### 5.1.4 Detection of others

Zhang et al. reported self-powered UVPD of p-n heterojunctions (TiO<sub>2</sub> NRs: C-CQDs/PTTh) consisting of p-type poly (2,2':5',2 Mobi'-trithiophene) (PTTh) and n-type coalbased CQDs sensitized TiO<sub>2</sub> nanorod arrays. 144 The formation mechanism of the p-n heterojunction is shown (Figure 3l-m). The self-powered UVPD generates numerous electron-hole pairs upon photoexcitation to increase the carrier concentration in TiO<sub>2</sub> NR. The electron-hole pairs are effectively separated by an internal electric field to realize self-powered detection. In addition, the p-n heterojunction will produce more photogenerated electron-hole pairs due to the energy level matching relationship formed between the TiO2 NRs sensitized by C-CQDs and the polymer PTTh with the strong absorption of C-CODs in the UV region. The

presence of the depletion layer between the p-n junctions inhibits the fast complexation of carriers. As a result, carrier transport and transfer in the heterojunction are improved by the sensitization of TiO2 nanorods by C-CQD, and the carrier lifetime is extended. The detection rate  $(D^*)$  and response rate (R) of the device were  $4.5 \times 10^{10}$  Jones and 1.45 mA/W at a light intensity of 0.35 mW/cm<sup>2</sup>, and the response times were 3.19 ms and 91.2 ms, respectively. Thus, the TiO2 NRs:C-CQDs/PTTh realizes high-performance selfpowered UVPD.

## 5.2 Biomedicine

In recent years, biomedical research has become more and more important as people become more and more concerned about health issues. Compared with conventional semiconductor quantum dots, coal-based CODs/GODs have attracted attention in biomedical fields such as biosensing and bioimaging due to their stable photoluminescence, high selectivity, high water solubility, low cytotoxicity, and biocompatibility. Biosensing can detect various biomolecules such as nucleic acids, enzymes and proteins. Yew et al. used coke-based GOD as a fluorescence resonance energy transfer receptor for the detection of DNA, with a detection limit of DNA concentration as low as 0.004 nM.<sup>64</sup> The wide linear detection range spanned three orders of magnitude and was determined to be 0.004-4 nM. Thus, coal-based GQDs are promising materials for the development of nanobiosensors capable of selective and highly sensitive DNA detection.

Some studies have utilized PEGylated liposomes encapsulating CQDs to improve the biocompatibility of oilsoluble CQDs. And animal experiments were carried out to investigate the feasibility of the prepared liposome-CODs for in vivo fluorescence imaging using HeLa loaded nude mice as an animal model.<sup>78</sup> The results showed that the prepared liposome-CQD maintained PL intensity in mice and could be used as a potentially excellent labeling material for in vivo and in vitro imaging (Figure 3n). Ghorai et al. verified that the low toxicity, biocompatibility and luminescent stability exhibited by coal-based GQD nanomaterials could make them potential probes for cancer therapy applications. 91 Coal-based GODs and their PEG-functionalized derivatives (PEG-GQDs) can also act as effective antioxidants. 123 Furthermore, H<sub>2</sub>O<sub>2</sub> reduction experiments were performed by bEnd to evaluate the protective ability of PEG-GQDs. The results showed that PEG-GQDs had better biostability and solubility and exhibited in vitro cytoprotective effects against H<sub>2</sub>O<sub>2</sub> even with delayed administration.

The coal-based CQDs/GQDs composites also showed good antimicrobial activity and antitoxicity. The Ag/CQD nanocomposites were found to inhibit the growth of both Gram-positive and Gram-negative bacteria by antimicrobial tests. 119 In addition, the negative surface charge (zeta potential of 1.91 mV) of Ag/COD nanocomposites can interact electrostatically with the positive charge of the bacterial cell wall more effectively. Generally, positively charged nanoparticles are more cytotoxic than negatively charged or neutral nanoparticles. Therefore Ag/CQD nanocomposites also exhibit antitoxicity. The continuous release of Ag<sup>+</sup> from Ag/CQD may be an effective way to kill microorganisms, thus ensuring its antimicrobial activity.

Although the research on the application of coal-based CODs/GODs to biomedical applications is still in its early stages, the scope of their application will be broadened with the rapid development of carbon point materials. In the future, the development and utilization of these CQDs/GQDs may revolutionize biomedical research.

## 5.3 Photocatalytic

Solar energy is the most readily available clean and sustainable energy source in nature. Efficient utilization of solar energy is a powerful strategy to solve the environmental crisis and energy shortage. Photocatalysis is expected to make important contributions in this regard. In recent years, CQDs/GQDs have gradually become a research hotspot as novel photocatalysts due to their excellent physicochemical properties. Firstly, CQDs/GQDs have excellent size effect and conductivity as 0D conducting materials. Secondly, the rich surface functional groups and excellent specific surface area of CQDs/GQDs exhibit a strong adsorption capacity for reactants, which is favorable for the photocatalytic reaction. And coal-based CQDs/GQDs show great potential in the fields of photocatalytic CO<sub>2</sub> reduction, photocatalytic hydrogen precipitation and photodegradation of pollutants due to their low cost, simple synthesis routes and excellent electron transfer efficiency. Table 1 summarizes the studies of coalbased CQDs/GQDs photocatalysts applied to photocatalytic.

Coal-based CQDs have been used for the photocatalytic degradation of 2-nitrophenol.<sup>66</sup> 2-nitrophenol acts as an activator and excites the deposition of electrons onto the CQDs. The CQDs acted as oxidizing and reducing agents in the degradation process. The active species generated during the photocatalytic reaction decompose 2-nitrophenol into non-toxic small molecules. Bai et al. applied asphaltenebased CDs for photocatalytic hydrogen production.<sup>94</sup> The increase in size favored the narrowing of the band gap width and the enhancement of the photo-absorption capacity.

Table 1: A summar	y of research on coal-based CC	Ds/GODs photocataly	sts applied to photocatalytic.

Photocatalyst	Carbon source	Target object	Synthesis method	Activity	Reference
CQDs; GNs	Subbituminous coal	2-Nitrophenols	Hydrothermal technique	80.79 %; 82.53 % (120 min)	66
CDs	Coal tar pitch	H <sub>2</sub> evolution	NaOH-assisted hydrothermal carbonization	60.75 mmol H <sub>2</sub> g <sup>-1</sup> h <sup>-1</sup>	94
CDs	Anthracite	Methylene blue; methyl orange	Selective oxidation of H <sub>2</sub> O <sub>2</sub>	0.135 min <sup>-1</sup> ; 0.115 min <sup>-1</sup> (16 min)	68
CQDs/TiO <sub>2</sub>	Lignite	Rhodamine B	In situ synthesize	Almost 95 % (180 min)	145
C-Dots/TiO <sub>2</sub>	Xinjiang Wucaiwan coal	Cotton pulp black liquor (COD <sub>cr</sub> removal rate)	Acid/ultrasonic mixed oxidation technique	81.2 % (3 h)	146
Ag/CDs	Xinjiang Wucaiwan coal	CO <sub>2</sub> reduction (CH <sub>3</sub> OH yield)	H <sub>2</sub> O <sub>2</sub> oxidation method	17.82 μmol h <sup>-1</sup> g <sup>-1</sup>	124
N-CDs/Cu NRs	Xinjiang Wucaiwan coal	Cotton pulp black liquor (COD <sub>cr</sub> removal rate)	Ammonia hydrothermal cutting method with hydrothermal method	94.33 % (60 min)	121

When the size of CDs was increased from 1.9 nm to 5.8 nm, the hydrogen precipitation efficiency increased by 70 %.

Coal-based CDs can exhibit rapid photocatalytic degradation of the organic dyes methylene blue and methyl orange under visible light.<sup>68</sup> Photocatalysis involves the generation of charge carriers and the associated catalytic reactions. The photogenerated carriers generated by CD upon photoexcitation separate and migrate to its surface and participate in the mineralization and degradation of organic pollutants. Significantly, the surface groups of CD can lead to different photocatalytic activities by inducing different energy trap levels. 147-149 And the surface energy trap level of CD is affected by the pH change of the reaction solution. Therefore, the change of pH affects the photodegradation efficiency of CD. The photocatalytic activity of CD for methylene blue degradation increased with increasing pH.

Since the fluorescence lifetime of CQDs/GQDs is only a few nanoseconds, the electrons and holes generated under photoexcitation tend to complex. Therefore, combining coalbased CQDs/GQDs with semiconductor catalysts into composites may be an effective strategy to broaden the visible light absorption range. An internal electric field can be formed between CQDs/GQDs and semiconductor catalysts to promote carrier separation and transfer and improve photocatalytic efficiency.

Coal-based CQD/TiO<sub>2</sub> heterostructured nanocomposites synthesized by in situ synthesis exhibit excellent photocatalytic activity under visible light. 145 This may be attributed to the following reasons: (1) the formation of Ti-O-C bonds at the CQD/TiO<sub>2</sub> heterojunction interface resulted in the narrowing of the bandgap with the red-shift of the absorption edge, which led to the improvement of the visible light utilization; (2) the CQDs acted as electron donors to realize the transfer of the photogenerated electrons to the

TiO<sub>2</sub> conduction band and participated in the degradation process; and (3) the separation of the photogenerated electron-hole pairs was improved by the heterojunction interface. C-Dots/TiO2 nanoparticles obtained by combining coal-based C-Dots with TiO2 particles can be used for degradation of pulping black liquor under visible light. 146 Compared with pure TiO<sub>2</sub>, the band gap of C-Dots/TiO<sub>2</sub> was reduced to 2.9 eV, and the PL intensity was significantly decreased. Most of the organic compounds in the pulping black liquor, except the nitrogen-containing heterocyclic compounds, were degraded after 3 h of light reaction.

Ag/CDs composites can be used for photocatalytic reduction of CO<sub>2</sub> to generate hydrocarbons. 124 The results showed that the main product of the photocatalytic reduction of CO<sub>2</sub> by Ag/CDs was CH<sub>3</sub>OH, and the CH<sub>3</sub>OH yield after 10 h of light exposure was increased by a factor of three compared with that of the pure Ag catalyst. When Ag interacted with CD, the photogenerated electrons on CD could be transferred to the Ag surface through the chemical bond between Ag and CD (Ag-O) or the interface between Ag and CD, which inhibited the complexation of photogenerated electrons and holes in CD (Figure 4a). And the photogenerated carriers generated by Ag nanoparticles under visible light irradiation can be separated by the SPR-induced localized electromagnetic field. The holes with high oxidizing ability of CD and the electrons with high reducing ability of Ag particles are involved in the reaction, respectively.

Sun et al. used the prepared N-CDs/Cu NRS nanocomposite catalysts for the photoelectron-catalytic degradation of CPBL and simultaneous hydrogen production. 121 The photoelectron-catalytic dual reaction occurred in an H-type photoreactor, in which the cathode produced H<sub>2</sub> and the anode degraded CPBL. The mechanism of N-CD/Cu NRs

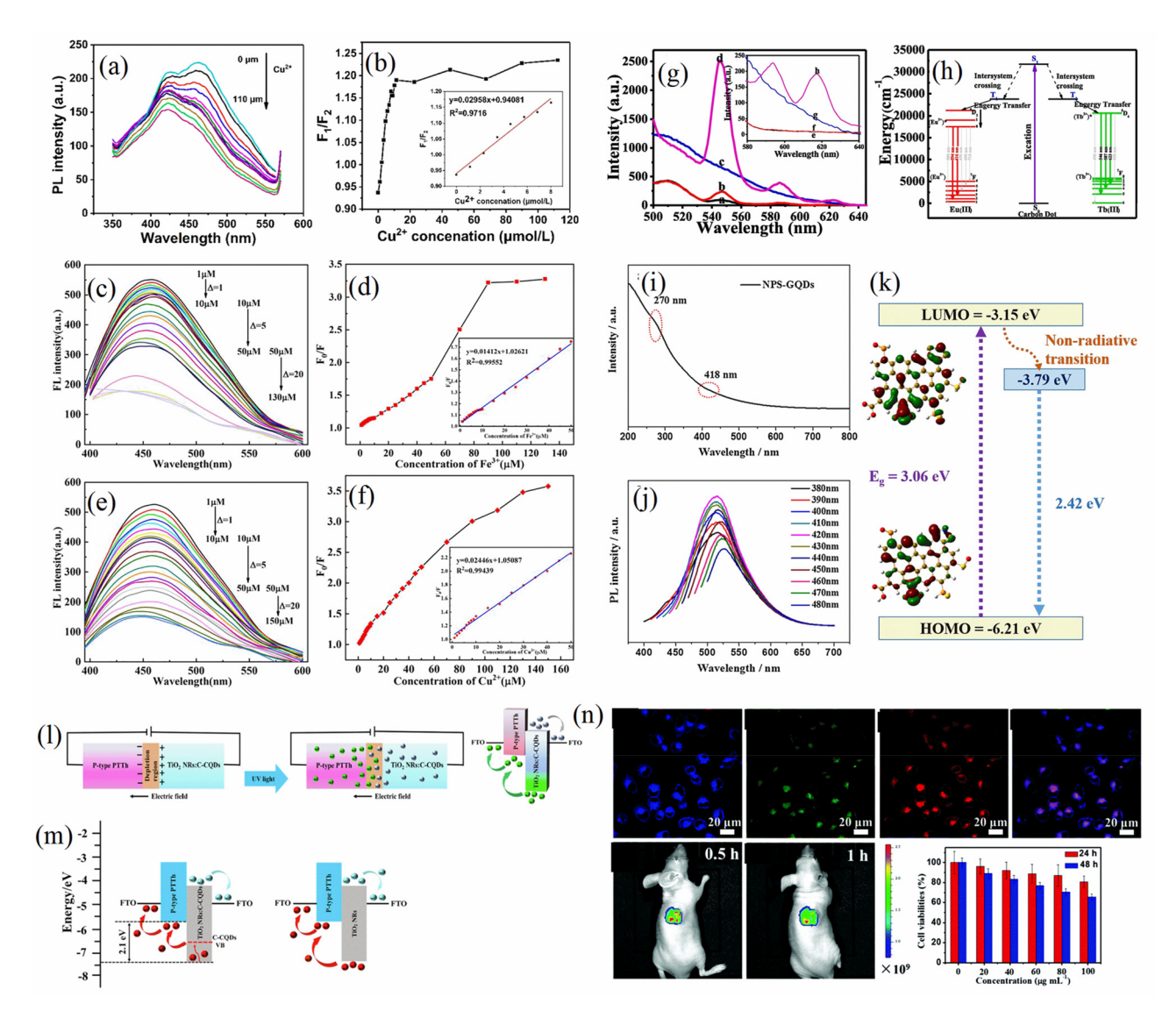


**Figure 4:** Application of various types of coal-based CDs. (a–b) Emission spectra of C-GQDs with Cu<sup>2+</sup> concentration in the range of 0~110 µM and fluorescence intensity ratios for different Cu<sup>2+</sup> concentrations;<sup>103</sup> (c–f) Fluorescence emission spectra of N-CQDs solutions with different Fe<sup>3+</sup> and Cu<sup>2+</sup> concentrations at 365 nm excitation wavelengths and the relationship between F<sub>0</sub>/F and Fe<sup>3+</sup> and Cu<sup>2+</sup> concentrations;<sup>127</sup> (g–h) Fluorescence spectra and energy level diagrams and energy transfer processes of Tb-CD systems in different fluorescence spectra and energy level schematic and energy transfer process of Tb-CD system in solution;<sup>62</sup> (i–k) UV absorption spectra, steady-state fluorescence spectra and fluorescence emission diagrams at different excitation wavelengths of NPS-GQDs;<sup>136</sup> (l–m) working mechanism and energy band diagrams of TiO<sub>2</sub> NRs:C-CQDs/PTTh p-n heterojunctions UVPDs;<sup>144</sup> (n) confocal fluorescence images of HeLa cells, *in vivo* fluorescence images of HeLa-loaded nude mice and cytotoxicity assessment of liposome-CQDs at higher doses at 405, 488 and 546 nm excitation.<sup>78</sup>

photoelectron-catalytic is shown (Figure 3d). Firstly, when N-CD/Cu NRs are exposed to light they can absorb electrons and induce the LSPR effect on the surface of Cu NRs, and the generated hot electrons will be transferred to the coal-based N-CD. Meanwhile, the N-CD region will also absorb photons to produce  $e^-$  and  $h^+$ . The reactive radicals oxidize CPBL into small non-toxic molecules. The  $e^-$  is transferred to the cathode under the applied bias pressure and forms  $H_2$  from the  $H^+$  crossing the proton exchange membrane. This study combines hydrogen production with wastewater treatment

and provides new ideas for the design of photoelectroncatalysis.

## **5.4 Electrocatalytic**

With the growing problems of energy shortage and environmental degradation, there is an increasing demand for stable and efficient energy conversion technologies. The development of electrocatalytic reactions has addressed this need to a certain extent, including hydrogen precipitation reaction (HER), oxygen precipitation reaction (OER), and oxygen reduction reaction (ORR). 150 However, the reaction kinetics of these non-homogeneous reactions behave slowly due to the multi-step electron transfer process, which has a limiting effect on the performance of the corresponding energetic devices. 151-154 To solve this problem, metal-free carbon-based oxygen reduction electrocatalysts have received attention from researchers. CQDs/GQDs as novel catalysts were introduced into the electrocatalytic process used to accelerate electrochemical reactions.

Zhao et al. prepared a highly active OER catalyst, QD-Ni<sub>x</sub>Fe<sub>y</sub>, by coordinating it with metal ions and annealing it using coal-based CQD as a precursor. 155 The x and v represent the Ni/Fe ratio. The high specific surface area provided by the carbon structure and the high electrical conductivity provided by the alloy nanoparticles enabled all the composites to exhibit a high electrochemically active surface area. The optimized metal ratios resulted in the optimal catalytic activity of QD-Ni<sub>92</sub>Fe<sub>8</sub>. In addition, the catalytic performance of QD-Ni<sub>92</sub>Fe<sub>8</sub> is more stable as the nanocatalyst embedded in the carbon matrix will exhibit better corrosion and solubility resistance. Lei et al. synthesized porous N-doped carbon nanosheets (PNCN) with defects and high graphitic nitrogen content using coal-based GODs as nitrogen and carbon sources and explored their ORR properties using a simple self-doping method. 43 The abundance of edge defects in coal-based GQDs contributes to the generation of large specific surface area PNCNs. The loose laminated structure of PNNs can also provide additional active sites and improve the mass transfer process of ORR. PCNs-900 (obtained at 900 °C) exhibited excellent ORR activity attributed to the synergistic effect of its graphitic nitrogen and high defect density. In addition, PCNs-900 exhibits high methanol tolerance and stability superior to commercial Pt/ C.

Hu et al. constructed an all carbon-based hybrid N-CD/G consisting of graphene surface-modified N-CD with significant electrocatalytic activity for ORR. 130 Comparison of the ORR onset potentials of each electrode yielded that the N-CD/G electrode was relatively more negative than the Pt/C electrode and more positive than the CD/G and rGO electrodes. And the oxygen reduction current density of the N-CD/G electrode was also much larger than that of the CD/G and rGO electrodes. Therefore, N-CDs play an important role in improving the electrocatalytic activity of the catalysts. The N-CD structure contains abundant defects and edge sites that favor ORR catalytic activity. The N-CD structure contains a large number of doped nitrogen atoms that can change the chemisorption mode of O2 and the electronic structure of CD and weaken O-O bonding, thus promoting the ORR of the

N-CD/G electrode. In particular, the stability of the N-CD/G electrode is superior to that of commercial Pt/C catalysts due to the strong interaction and good compatibility between the graphene carrier and N-CD. Fei et al. found that hybridized nanosheets BN-GQD/G exhibited excellent ORR activity. 131 BN-GOD/G was prepared by self-assembly of N- and B-codoped coal-based GQDs on graphene. In particular, the ORR activity was affected by dopant concentration and doping time. The ORR activity decreased with increasing doping time. Lower BN doping leads to a lower number of electrocatalytic sites. Whereas higher BN doping content would yield B and N dopant pairs with no promoting effect on ORR activity.

## 5.5 Energy storage

Research has shown that CQDs/GQDs can significantly improve the storage efficiency and energy conversion of various energy storage devices, including solar cells (SCs), supercapacitors, rechargeable batteries, and light-emitting diodes (LEDs), among others.

In the field of LEDs, CQDs/GQDs are considered as an ideal alternative to traditional semiconductor quantum dot phosphors and rare earth phosphors due to their tunable fluorescence, wide visible light range, and low toxicity and river cost. Feng et al. prepared white LEDs by combining CQDs synthesized with coke as a carbon source as a white light converter with a UV chip.<sup>74</sup> The color temperature (5125 K) and color product coordinates (0.31, 0.35) of the CQD-based LEDs were located in the cool white light region. And the CQD-based LEDs showed good stability in continuous light illumination at 3.2 V for 4 h, which is promising for application in light-emitting devices.

Incorporation of QDs into polymer matrices is also an effective means to enhance their applications in fields such as photovoltaics. Polymers can slow down the agglomeration of QDs and thus ensure their emission properties, and they can act as matrices to provide chemical and mechanical stability to the composites on the other hand. Polymer luminescent composites PVA/GQDs can be prepared by aqueous solution casting method using coal-based GQDs as raw materials. 156 The solid-state fluorescence exhibited by the polymer luminescent film was attributed to the fluorescent properties of the coal-based GQD. The photoluminescence intensity of the composites was maximized at a GQD content of 10 wt%, and the optical transparency was higher at a GQD content of 1-5 wt% (78-91%). The PL spectrum of the PVA/GQD nanocomposites is broad and covers most of the visible light range, so there is a great potential for its application as a luminescent body for white light LEDs.

Supercapacitors are widely used in electronic equipment and automotive industries, among others, due to their long cycle life, fast charging and discharging, and high power density. Carbon material capacitors have excellent cycle stability and multiplicity performance at high current density. Improving the volumetric capacitance of carbon electrode materials has become an important means to address the current lightweighting and miniaturization of devices. 157,158 However, carbon materials face the contradiction between high density, abundant pores and large specific surface area. The preparation of carbon materials that can overcome these contradictions remains difficult. Coal-based carbon nanomaterials have gradually come into the limelight as efficient electrode materials for supercapacitors. Oin et al. constructed microporous carbon with high density (0.86 g cm<sup>-3</sup>) and high specific surface area (1,345 m<sup>2</sup> g<sup>-1</sup>) by homogeneously activating CDs synthesized with coal liquefaction residue as the carbon source. 90 The abundant functional groups, smaller size structure and highly conjugated nuclei of CD facilitate the construction of porous carbon structures. Microporous carbon provides high weight and volume capacitance for supercapacitors exhibiting good multiplicity performance. CD was also used as a functional enhancement phase embedded in electrostatically spun CNFs. The viscosity of the spinning solution determines the morphology of the electrostatically spun nanofibers. CD with abundant functional groups exhibited strong interactions with polyacrylonitrile molecules thereby increasing the fiber diameter. As a result, the activated RCNF balanced the contradiction between the porous structure and the strong carbon skeleton and exhibited high capacitive energy storage properties, high flexibility, high mechanical strength and high specific surface area  $(1.921 \text{ m}^2 \text{ g}^{-1})$ .

Zhang et al. prepared hierarchical porous carbon nanosheets (HPCNs) and used them as electrodes for supercapacitors by a template-assisted assembly strategy using coal-based GQDs as building blocks. 159 The HPCNs exhibit interconnected loosely stacked graphene structures with abundant active centers, excellent electrical conductivity, and sufficient ion migration channels. Therefore, HPCNs are suitable for electrodes of high-performance supercapacitors. The capacitive performance of AHHPCNs after in situ activation by adding a small amount of KOH was greatly improved, exhibiting a high specific capacitance of  $230 \,\mathrm{F \,g^{-1}}$  and a capacitance retention of  $170 \,\mathrm{F \,g^{-1}}$ . The improved electrochemical performance of AHPCN can be attributed to the fact that the expansion of the mesopore volume provides more ionic channels than that of HPCN, while the increased microporosity and larger specific surface area provide more energy storage sites.

Lithium-ion batteries (LIBs) have become the preferred choice in the new energy era due to their low cost, environmental friendliness, excellent cycling stability, and ultrafast charging and discharging rates. Graphite is an ideal anode material due to its low price, abundant lithium-ion storage sites and high crystallinity. However, the low theoretical capacity of traditional commercial graphite cannot meet the demand of next-generation energy storage systems. Therefore, the development of novel anode materials is important to realize the high electrochemical performance of LIB. Shi et al. prepared porous carbon frameworks by carbonizing coal-based CQD powders via N2 atmosphere under elevated temperature conditions, achieving a directional transition from 0-dimensional CQDs to 3-dimensional porous carbon skeletons.<sup>92</sup> The prepared porous carbon frameworks consisted of twisted and cross-linked nanosheets exhibiting mesoporous/microporous gradient distribution of porous level structure and good specific surface area, which can be used as anode materials for LIBs. The crystallinity of the porous carbon skeleton increased with increasing carbonization temperature and the presence of defects and disordered cross sections decreased. In particular, the porosity level of the porous carbon framework was also affected by the carbonization temperature. The larger pore volume and specific surface area facilitated electrodeelectrolyte interactions, providing sufficient space and active sites for Li<sup>+</sup> storage. In addition, the gradientdistributed porous level structure also promotes rapid Li<sup>+</sup> transport, which improves the electrochemical performance. As a result, LIBs with porous carbon frameworks as anode materials exhibited excellent long-term electrochemical stability, achieving a maximum reversible capacity of 402 mA h/g at 100 mA/g (Figure 5b-e). Even after undergoing 1.000 cycles at 2.000 mA/g, it maintained a reversible capacity of 273 mA h/g. Therefore, the development and utilization of coal-based carbon materials have great potential for lithium storage.

C-GQDs/α-Fe<sub>2</sub>O<sub>3</sub> composites prepared by secondary electrodeposition using coal-based GQDs as electrolyte can be used as anode materials for LiBs. 161 The specific capacitance of the C-GQDs/α-Fe<sub>2</sub>O<sub>3</sub> composites reached 1,582.5 mA h/g at a current density of 1 A/g and 1,091 mA h/g at a high current density (5 A/g), which exhibited good multiplicative and cycling performance (Figure 51–0). The α-Fe<sub>2</sub>O<sub>3</sub> in the composite maintains a unique antler-like structure. The C-GQD loading creates a "bridge effect" between the antler-shaped skeletons and protects the numerous pores in the skeletons. This porous structure promotes rapid Li<sup>+</sup> transport and improves the conductivity of the material. In addition, the continuous C-GQD network structure not only effectively buffers the volume expansion

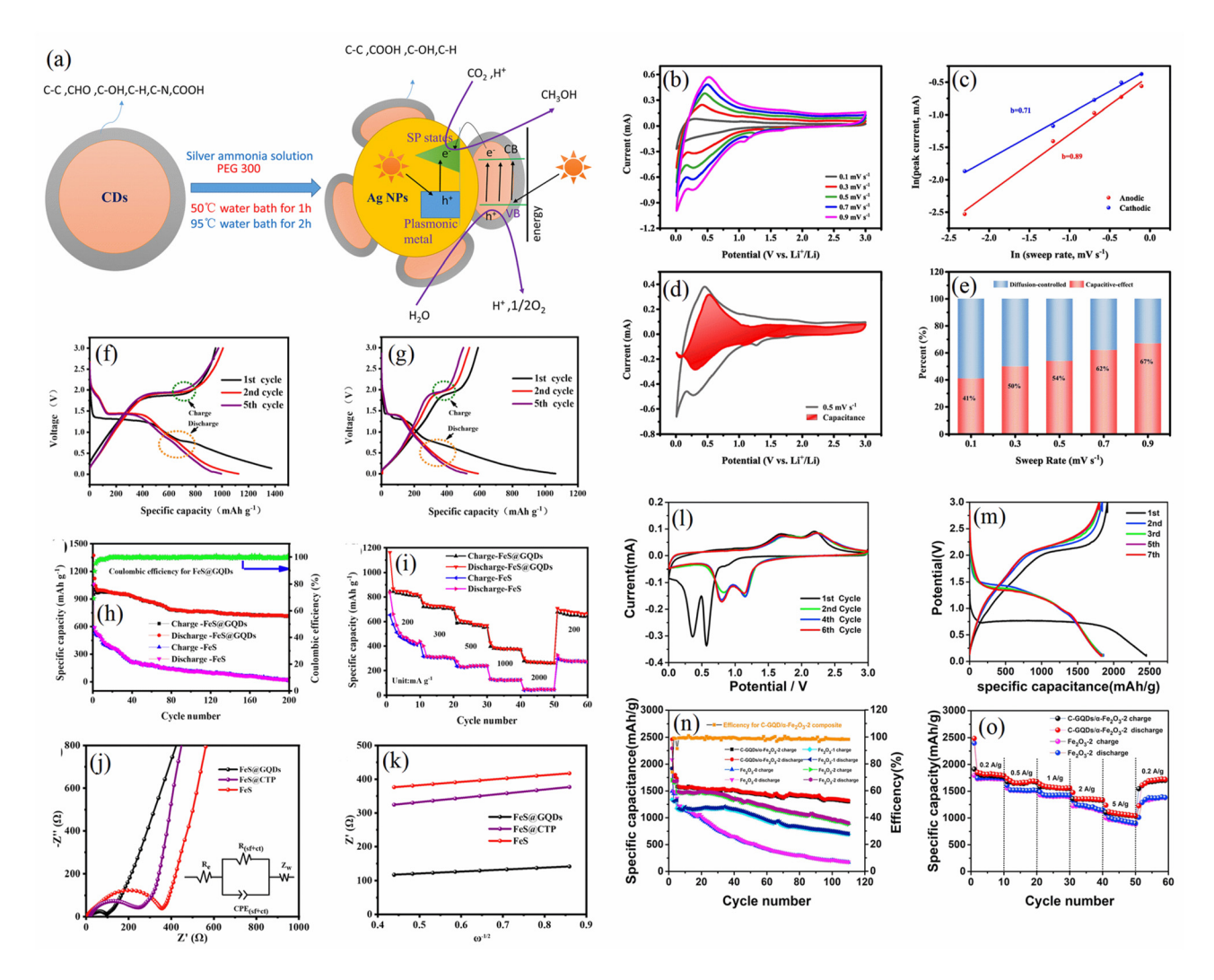


Figure 5: Application of various types of coal-based CDs. (a) Formation mechanism of Ag/CDs and CO<sub>2</sub> reduction mechanism, 124 (b-e) CV curves of PCF-700 at different scan rates, linear relationship between lni and lnv, contribution of capacitance at 0.5 mV s<sup>-1</sup> and percentage of capacitance effect contribution and diffusion control contribution at different scan rates; 92; (f-k) constant current discharge conditions, charge curves of FeS@GQDs and FeS at 100 mA g<sup>-1</sup>, cycling performance at 100 mA g<sup>-1</sup> current density for 200 cycles, rate capability and electrochemical impedance spectra of FeS@GQDs, FeS, and FeS@CTP at different current densities, inverse of impedance (Z') versus angular frequency ( $\omega$ ) square root between the fitted lines; <sup>160</sup> cyclic voltammograms of (I-o)C-GQDs/α-Fe<sub>2</sub>O<sub>3</sub>-2 at 0.1 mV/s, constant-current charge/discharge curves at 0.2 A/g, cyclic performance curves and coulombic efficiency, and rate-performance curves of Fe<sub>2</sub>O<sub>3</sub>-2 with the composites.<sup>161</sup>

during charging and discharging, but also prevents the direct contact between Fe<sub>2</sub>O<sub>3</sub> and the electrolyte, thus maintaining the structural integrity of the composite.

GQDs in close contact with FeS nanoparticles can form FeS@GQD strongly coupled composite electrode materials. 160 The bud-like morphology of FeS@GQD can be observed with many folds at larger magnification. These folds act as lithium storage sites and channels, and their surfaces can flexibly inhibit the volume expansion during electrochemical processes and thus limit the rapid decay of the battery capacity from the finishing. When evaluated as an anode material for LIBs, the FeS@GQD composites exhibit

higher initial coulombic efficiency and better rate performance than pure FeS (Figure 5f-k). An excellent reversible capacity of 718.7 mAh g<sup>-1</sup> was provided after 200 cycles at 100 mA g<sup>-1</sup>. The excellent electrochemical properties of FeS@GQD were attributed to the successful coupling between GQD and FeS through the formation of C-S-C. This synergistic interaction provides good porosity and large specific surface area, resulting in improved conductivity and enhanced structural stability.

Chalcogenide solar cells have received wide attention in recent years. Optimizing the interfacial properties between carbon electrode and chalcogenide is a key means to

improve the photovoltaic conversion efficiency of carbonbased chalcogenide solar cells. Hu et al. used coal-based N-GQDs to improve the photovoltaic performance of chalcogenide. 120 The electron deficient structure of Pb2+ can be used as Lewis acid and N-GOD can be used as Lewis base. The electron-rich pyridine nitrogen in N-GQD forms coordination bonds with uncoordinated lead ions by sharing electron pairs, thus reducing the hole trap density and passivating the Pb<sup>2+</sup> defects. The non-radiative complexation of the chalcogenide films was greatly reduced due to the passivation of N-GQD and the long-term stability was improved.

Polyacrylonitrile-derived electrostatically spun carbon nanofiber fabrics (ECNFs) have shown great potential in many fields such as flexible energy storage materials and smart membranes due to their sufficient flexibility and mechanical strength. 162-164 However, the limited flexibility and strength restrict their practical applications. Zhu et al. found that the incorporation of coal-based GODs (CGQDs) into the spinning solution could significantly improve the flexibility, Young's modulus and tensile strength of ECNFs. 165 Compared with pure polyacrylonitrile-derived ECNFs, the Young's modulus of ECNFs incorporating CGQDs increased more than sevenfold. The cross-linking effect of the introduced CGQD is believed to be responsible for the improved performance of ECNF. The abundant oxygen-containing functional groups and good chemical reactivity on CGQD can act as cross-linking agents and form a flexible, strong and dense carbon skeleton. In addition, the hydrophobicity of ECNF gradually increases with the increase of CGQD content due to the increase of carbon nanofiber diameter. The optimized ECNF exhibits a contact angle of 142 and can also be used for durable and efficient gravity-driven oil/water separation.

## 6 Conclusions and outlook

The traditional coal processing industry has low efficiency and limitations. The development and research of CQDs/ GQDs offer new prospects for low-carbon processing and clean utilization of coal. This paper reviews the synthetic methods and physicochemical properties of CQDs/GQDs prepared from coal and its derivatives, focusing on the formation mechanism of coal-based CODs/GODs and their functionalization. The coal-based CQDs/GQDs synthesized by different preparation processes and different carbonaceous precursors will have different microstructures, electron transfer capabilities and photoluminescent properties. Structural analysis is used to assist in understanding the formation mechanism of coal-based CQDs/GQDs, including acid etching and oxidation, acid-free oxidation, carbonation,

physical bond breaking, oxidative functionalization, and electrochemical stripping. The three main functionalization strategies of coal-based CQDs/GQDs are surface modification, hybridization with other materials and heteroatom doping. In addition, the applications of coal-based CQDs/ GODs in sensing, photocatalysis, electrocatalysis, energy storage and biomedicine are discussed. Although significant progress has been made in the synthesis and application of coal-based CQDs/GQDs in recent years, there are still several issues that deserve further investigation.

- Existing studies have shown that the structures and properties of coal-based CQDs/GQDs are largely influenced by the structures of carbonaceous precursors. And the structure of carbonaceous precursors can be tuned by molecular tailoring strategy. Therefore, functional carbon materials with specific structures and properties can be prepared by tuning coal and its derivatives with different degrees of graphitization.
- (2) There are many inferences about the photoluminescence mechanism and formation mechanism of coal-based CODs/GODs. Unfortunately, the mechanisms associated with coal-based CQDs/GQDs are still difficult to explain clearly due to their unclear chemical structures and surface moieties as well as insufficient characterization means. It is hoped that more advanced characterization means such as in situ techniques will be used to provide a theoretical and technical basis for understanding the structure and properties of coal-based CQDs/GQDs.
- At this stage, the research mainly focuses on the syn-(3) thesis strategy and the modulation of the surface structure. Therefore, it is necessary to understand the evolutionary mechanism of coal and its derivatives to carbon materials in more detail at the molecular or atomic level.
- (4) Compared with semiconductor QDs and other carbon materials, research on coal-based CQDs/GQDs is still in its infancy. There are still some unknown properties of coal-based CQDs/GQDs that have not yet been investigated, and the structure-property relationship about is not well elucidated at present. Their nanoscale physical and chemical properties have not been accurately defined, thus limiting their application in the energy field.
- (5) Coal-based CQDs/GQDs have great potential for application in many fields. Unfortunately, coal-based CQDs/ GQDs have not been put into practical applications at present, and their mechanism of action in various applications has not been well explained. Large-scale production of coal-based CQDs/GQDs remains a challenge in terms of cost, quality and environmental

impact. Therefore, the development of coal-based CQDs/GQDs in more fields and their application in practical production can be promoted through indepth investigation of their structures and properties.

In summary, more pioneering work is needed in the largescale preparation and application of coal-based CQDs/GQDs. Hopefully, this content will further enrich carbon science and coal chemistry, provide important information for designing efficient coal-based carbon nanomaterials and offer sustainable options for overcoming bottlenecks in coal applications.

**Research ethics:** Not applicable. **Informed consent:** Not applicable.

Author contributions: All authors have accepted responsibility for the entire content of this manuscript and approved its submission.

Use of Large Language Models, AI and Machine Learning Tools: None declared.

**Conflict of interest:** The authors state no conflict of interest. Research funding: National Natural Science Foundation of China (Grant No. 52174262, and 52304299), National Key R&D Program of China (2021YFC2902604), Joint Fund for Science and Technology R&D Programs of Henan Province (222301420036), China Postdoctoral Science Foundation (2022M712881), Natural Science Foundation of Henan Province (252300421089), Training Program Project for University Youth Key Teacher of Henan Province (2024GGJS009).

Data availability: Not applicable.

## References

- 1. Fernando, K. A. S.; Sahu, S.; Liu, Y.; Lewis, W. K.; Guliants, E. A.; Jafariyan, A.; Wang, P.; Bunker, C. E.; Sun, Y. P. Carbon Quantum Dots and Applications in Photocatalytic Energy Conversion. ACS Appl. Mater. Inter. 2015, 7 (16), 8363-8376.
- 2. Rasal, A. S.; Yadav, S.; Yadav, A.; Kashale, A. A.; Manjunatha, S. T.; Altaee, A.; Chang, J. Y. Carbon Quantum Dots for Energy Applications: A Review. ACS Appl. Nano Mater. 2021, 4 (7), 6515-6541.
- 3. Ozkan, M. Quantum Dots and Other Nanoparticles: what Can They Offer to Drug Discovery? *Drug Discov. Today* **2004**, *9* (24), 1065–1071.
- 4. Warburton, R. J. Self-assembled Semiconductor Quantum Dots. Contemp. Phys. 2002, 5 (43), 351-364.
- 5. Cao, L.; Wang, X.; Meziani, M. J.; Lu, F.; Wang, H.; Luo, P. G.; Lin, Y.; Harruff, B. A.; Veca, L. M.; Murray, D.; Xie, S. Y.; Sun, Y. P. Carbon Dots for Multiphoton Bioimaging. J. Am. Chem. Soc. 2007, 129 (37), 11318-11319.
- 6. Larson, D. R.; Zipfel, W. R.; Williams, R. M.; Clark, S. W.; Bruchez, M. P.; Wise, F. W.; Webb, W. W. Water-soluble Quantum Dots for Multiphoton Fluorescence Imaging In Vivo. Science 2003, 300 (5624), 1434-1436.

- 7. Xu, X.; Ray, R.; Gu, Y.; Ploehn, H. J.; Gearheart, L.; Raker, K.; Scrivens, W. A. Electrophoretic Analysis and Purification of Fluorescent Single-Walled Carbon Nanotube Fragments. J. Am. Chem. Soc. 2004, 126 (40), 12736-12737.
- 8. Mai, X.; Thi Kim Chi, T.; Nguyen, T.; Ta, V. Scalable Synthesis of Highly Photoluminescence Carbon Quantum Dots. Mater. Lett. 2020, 268,
- 9. Devi, P.: Saini, S.: Kim, K. H. The Advanced Role of Carbon Quantum Dots in Nanomedical Applications. Biosens. Bioelectron. 2019, 141, 111158.
- 10. Li, Q.; Zhou, M.; Yang, M.; Yang, Q.; Zhang, Z.; Shi, J. Induction of Long-Lived Room Temperature Phosphorescence of Carbon Dots by Water in Hydrogen-Bonded Matrices. Nat. Commun. 2018, 9 (1), 734.
- 11. Tang, I.; Kong, B.; Wu, H.; Xu, M.; Wang, Y.; Wang, Y.; Zhao, D.; Zheng, G. Carbon Nanodots Featuring Efficient FRET for Real-Time Monitoring of Drug Delivery and Two-Photon Imaging. Adv. Mater. **2013**, 25 (45), 6569-6574.
- 12. Xie, Z.; Wang, F.; Liu, C. Y. Organic-Inorganic Hybrid Functional Carbon Dot Gel Glasses. Adv. Mater. 2012, 24 (13), 1716–1721.
- 13. Zhang, W. F.; Zhu, H.; Yu, S. F.; Yang, H. Y. Observation of Lasing Emission from Carbon Nanodots in Organic Solvents. Adv. Mater. 2012, 24 (17), 2263-2267.
- 14. Zheng, M.; Liu, S.; Li, J.; Qu, D.; Zhao, H.; Guan, X.; Hu, X.; Xie, Z.; Jing, X.; Sun, Z. Integrating Oxaliplatin with Highly Luminescent Carbon Dots: An Unprecedented Theranostic Agent for Personalized Medicine. Adv. Mater. 2014, 26 (21), 3554-3560.
- 15. Han, M.; Zhu, S.; Lu, S.; Song, Y.; Feng, T.; Tao, S.; Liu, J.; Yang, B. Recent Progress on the Photocatalysis of Carbon Dots: Classification, Mechanism and Applications. Nano Today 2018, 19, 201–218.
- 16. Jia, H.; Wang, Z.; Yuan, T.; Yuan, F.; Li, X.; Li, Y.; Tan, Z.; Fan, L.; Yang, S. Electroluminescent Warm White Light-Emitting Diodes Based on Passivation Enabled Bright Red Bandgap Emission Carbon Quantum Dots. Adv. Sci. 2019, 6 (13), 1900397.
- 17. Luo, Z.; Qi, G.; Chen, K.; Zou, M.; Yuwen, L.; Zhang, X.; Huang, W.; Wang, L. Microwave-Assisted Preparation of White Fluorescent Graphene Quantum Dots as a Novel Phosphor for Enhanced White-Light-Emitting Diodes. Adv. Funct. Mater. 2016, 26 (16),
- 18. Qu, S.; Zhou, D.; Li, D.; Ji, W.; Jing, P.; Han, D.; Liu, L.; Zeng, H.; Shen, D. Toward Efficient Orange Emissive Carbon Nanodots through Conjugated sp<sup>2</sup>-Domain Controlling and Surface Charges Engineering. Adv. Mater. 2016, 28 (18), 3516-3521.
- 19. Chen, Y.; Zheng, M.; Xiao, Y.; Dong, H.; Zhang, H.; Zhuang, J.; Lei, B.; Liu, Y. A Self-Quenching-Resistant Carbon-Dot Powder with Tunable Solid-State Fluorescence and Construction of Dual-Fluorescence Morphologies for White Light-Emission. Adv. Mater. 2016, 28 (2), 312-318.
- 20. Lingam, K.; Podila, R.; Qian, H.; Serkiz, S.; Rao, A. M. Evidence for Edge-State Photoluminescence in Graphene Quantum Dots. Adv. Funct. Mater. 2013, 23 (40), 5062-5065.
- 21. Briscoe, J.; Marinovic, A.; Sevilla, M.; Dunn, S.; Titirici, M. Biomass-Derived Carbon Quantum Dot Sensitizers for Solid-State Nanostructured Solar Cells. Angew. Chem. Int. Ed. 2015, 54 (15), 4463-4468.
- 22. Sekiya, R.; Uemura, Y.; Murakami, H.; Haino, T. White-Light-Emitting Edge-Functionalized Graphene Quantum Dots. Angew. Chem. Int. Ed. **2014**, *53* (22), 5619-5623.
- 23. Zhu, S.; Zhang, J.; Tang, S.; Qiao, C.; Wang, L.; Wang, H.; Liu, X.; Li, B.; Li, Y.; Yu, W.; Wang, X.; Sun, H.; Yang, B. Surface Chemistry Routes to Modulate the Photoluminescence of Graphene Quantum Dots: From

- Fluorescence Mechanism to Up-Conversion Bioimaging Applications. Adv. Funct. Mater. 2012, 22 (22), 4732-4740.
- 24. Zheng, M.; Xie, Z.; Qu, D.; Li, D.; Du, P.; Jing, X.; Sun, Z. On-Off-On Fluorescent Carbon Dot Nanosensor for Recognition of Chromium(VI) and Ascorbic Acid Based on the Inner Filter Effect. ACS Appl. Mater. Inter. 2013, 5 (24), 13242-13247.
- 25. Huang, J. J.; Zhong, Z. F.; Rong, M. Z.; Zhou, X.; Chen, X. D.; Zhang, M. Q. An Easy Approach of Preparing Strongly Luminescent Carbon Dots and Their Polymer Based Composites for Enhancing Solar Cell Efficiency. Carbon 2014, 70, 190-198.
- 26. Li, H.; He, X.; Liu, Y.; Huang, H.; Lian, S.; Lee, S.; Kang, Z. One-step Ultrasonic Synthesis of Water-Soluble Carbon Nanoparticles with Excellent Photoluminescent Properties. Carbon 2011, 49 (2), 605-609.
- 27. Zhu, H.; Wang, X.; Li, Y.; Wang, Z.; Yang, F.; Yang, X. Microwave Synthesis of Fluorescent Carbon Nanoparticles with Electrochemiluminescence Properties. Chem. Commun. 2009 (34), 5118; https://doi.org/10.1039/b907612c.
- 28. Wen, X.; Yu, P.; Toh, Y.; Lee, Y.; Hsu, A.; Tang, J. Near-infrared Enhanced Carbon Nanodots by Thermally Assisted Growth. Appl. Phys. Lett. 2012, 101 (16), 163107.
- 29. Lim, S. Y.; Shen, W.; Gao, Z. Carbon Quantum Dots and Their Applications. Chem. Soc. Rev. 2015, 44 (1), 362-381.
- 30. Wang, R.; Lu, K.; Tang, Z.; Xu, Y. Recent Progress in Carbon Quantum Dots: Synthesis, Properties and Applications in Photocatalysis. J. Mater. Chem.. A, Mater. Energy Sustain. 2017, 5 (8), 3717-3734.
- 31. Wang, Y.; Hu, A. Carbon Quantum Dots: Synthesis, Properties and Applications. J. Mater. Chem. C 2014, 2 (34), 6921-6939.
- 32. Tian, R.; Zhong, S.; Wu, J.; Jiang, W.; Shen, Y.; Jiang, W.; Wang, T. Solvothermal Method to Prepare Graphene Quantum Dots by Hydrogen Peroxide. Opt. Mater. 2016, 60, 204-208.
- 33. Höök, M.; Zittel, W.; Schindler, J.; Aleklett, K. Global Coal Production Outlooks Based on a Logistic Model. Fuel 2010, 89 (11), 3546-3558.
- 34. Moothi, K.; Iyuke, S. E.; Meyyappan, M.; Falcon, R. Coal as a Carbon Source for Carbon Nanotube Synthesis. Carbon 2012, 50 (8), 2679-2690.
- 35. Oin, Z. New Advances in Coal Structure Model. Int. I. Min. Sci. Techno. 2018, 28 (4), 541-559.
- 36. Ma, X.; Dong, X.; Fan, Y. Prediction and Characterization of the Microcrystal Structures of Coal with Molecular Simulation. Energ. Fuel **2018**, *32* (3), 3097–3107.
- 37. Pang, L. S. K.; Vassallo, A. M.; Wilson, M. A. Fullerenes from Coal. Nature 1991, 352 (6335), 480.
- 38. Guo, J.; Guo, M.; Jia, D.; Song, X.; Tong, F. CdS Loaded on Coal Based Activated Carbon Nanofibers with Enhanced Photocatalytic Property. Chem. Phys. Lett. 2016, 659, 66-69.
- 39. Wang, G.; Wang, X.; Sun, J.; Zhang, Y.; Hou, L.; Yuan, C. Porous Carbon Nanofibers Derived from Low-softening-point Coal Pitch towards All-Carbon Potassium Ion Hybrid Capacitors. Rare Met. 2022, 41 (11), 3706-3716.
- 40. Das, T.; Chauhan, H.; Deka, S.; Chaudhary, S.; Boruah, R.; Saikia, B. K. Promising Carbon Nanosheet-Based Supercapacitor Electrode Materials from Low-Grade Coals. Micropor. Mesopor. Mat. 2017, 253,
- 41. Awati, A.; Maimaiti, H.; Wang, S.; Xu, B. Photo-derived Fixation of Dinitrogen into Ammonia at Ambient Condition with Water on Ruthenium/coal-Based Carbon Nanosheets. Sci. Total Environ. 2019, 695, 133865.
- 42. Gan, X.; Yuan, R.; Zhu, J.; Li, Q.; Tang, T.; Qin, F.; Zhu, L.; Zhang, J.; Wang, L.; Zhang, S.; Song, H.; Jia, D. Ultra-fine Carbon Nanosheets from Coal

- Oxidation for Tri-functional Improvement of Carbon Nanofiber Fabrics. Carbon 2023, 201, 381-389.
- 43. Das, T.; Saikia, B. K. Nanodiamonds Produced from Low-Grade Indian Coals. ACS Sustain. Chem. Eng. 2017, 5 (11), 9619-9624.
- 44. B, M.; Raj, A. M.; Chirayil, G. T. Tunable Direct Band Gap Photoluminescent Organic Semiconducting Nanoparticles from Lignite. Sci. Rep.-UK 2017, 7 (1), 19012.
- 45. B, M.; Raj, A. M.; Thomas, G. C. Tailoring of Low Grade Coal to Fluorescent Nanocarbon Structures and Their Potential as a Glucose Sensor. Sci. Rep.-UK 2018, 8 (1), 13891.
- 46. Dedong, Z.; Maimaiti, H.; Awati, A.; Yisilamu, G.; Fengchang, S.; Ming, W. Synthesis and Photocatalytic CO<sub>2</sub> Reduction Performance of Cu<sub>2</sub>O/ Coal-Based Carbon Nanoparticle Composites. Chem. Phys. Lett. 2018, 700, 27-35.
- 47. Yin, F.; Lu, K.; Wei, X.; Fan, Z.; Li, J.; Kong, Q.; Zong, Z. M.; Bai, H. C. Fabrication of N/O Self-Doped Hierarchical Porous Carbons Derived from Modified Coal Tar Pitch for High-Performance Supercapacitors. Fuel 2022, 310, 122418.
- 48. Zhu, Y.; Wang, Y.; Wang, T.; Liu, H.; Liu, H.; Zang, M. One-step Preparation of Coal-Based Magnetic Activated Carbon with Hierarchically Porous Structure and Easy Magnetic Separation Capability for Adsorption Applications. J. Magn. Magn Mater. 2023, 569, 170480.
- 49. Xu, H.; Lin, Q.; Zhou, T.; Chen, T.; Lin, S.; Dong, S. Facile Preparation of Graphene Nanosheets by Pyrolysis of Coal-Tar Pitch with the Presence of Aluminum. J. Anal. Appl. Pyrol. 2014, 110, 481-485.
- 50. Zhang, L.; Hui, K. N.; Hui, K. S.; Lee, H. Facile Synthesis of Porous CoAl-Layered Double Hydroxide/graphene Composite with Enhanced Capacitive Performance for Supercapacitors. Electrochim. Acta 2015, 186, 522-529.
- 51. Zhang, C.; Xie, Y.; Zhang, C.; Lin, J. Upgrading Coal to Multifunctional Graphene-Based Materials by Direct Laser Scribing. Carbon 2019, 153,
- 52. Li, H.; He, X.; Wu, T.; Jin, B.; Yang, L.; Qiu, J. Synthesis, Modification Strategies and Applications of Coal-Based Carbon Materials. Fuel Process. Technol. 2022, 230, 107203.
- 53. Cai, T.; Liu, B.; Pang, E.; Ren, W.; Li, S.; Hu, S. A Review on the Preparation and Applications of Coal-Based Fluorescent Carbon Dots. New Carbon Mater. 2020, 35 (6), 646-666.
- 54. Li, K.; Liu, G.; Zheng, L.; Jia, J.; Zhu, Y.; Zhang, Y. Coal-derived Carbon Nanomaterials for Sustainable Energy Storage Applications. New Carbon Mater. 2021, 36 (1), 133-154.
- 55. Hoang, V. C.; Hassan, M.; Gomes, V. G. Coal Derived Carbon Nanomaterials - Recent Advances in Synthesis and Applications. Appl. Mater. Today 2018, 12, 342-358.
- 56. Du, M.; Advincula, P. A.; Ding, X.; Tour, J. M.; Xiang, C. Coal-Based Carbon Nanomaterials: En Route to Clean Coal Conversion toward Net Zero CO<sub>2</sub>. Adv. Mater. 2023, 35 (25), e2300129.
- 57. He, Z.; Liu, S.; Zhang, C.; Fan, L.; Zhang, J.; Chen, Q.; Sun, Y.; He, L.; Wang, Z.; Zhang, K. Coal Based Carbon Dots: Recent Advances in Synthesis, Properties, and Applications. Nano select 2021, 2 (9), 1589-1604
- 58. Hou, Q.; Xing, B.; Guo, H.; Kang, W.; Yi, G.; Cheng, S.; Zhang, C.; Zhang, Y. Application of Coal-Based Carbon Dots for Photocatalysis and Energy Storage: a Minireview. New J. Chem. 2022, 46 (36),
- 59. Chandra, S.; Laha, D.; Pramanik, A.; Ray Chowdhuri, A.; Karmakar, P.; Sahu, S. K. Synthesis of Highly Fluorescent Nitrogen and Phosphorus Doped Carbon Dots for the Detection of Fe<sup>3+</sup> Ions in Cancer Cells. Luminescence 2016, 31 (1), 81-87.

- 60. Mohapatra, S.; Sahu, S.; Sinha, N.; Bhutia, S. K. Synthesis of a Carbon-Dot-Based Photoluminescent Probe for Selective and Ultrasensitive Detection of Hq<sup>2+</sup> in Water and Living Cells. The Analyst 2015, 140 (4), 1221-1228.
- 61. Li, F.; Liu, C.; Yang, J.; Wang, Z.; Liu, W.; Tian, F. Mg/N Double Doping Strategy to Fabricate Extremely High Luminescent Carbon Dots for Bioimaging. RSC Adv. 2014, 4 (7), 3201-3205.
- 62. Chu, X.; Chen, T.; Cao, Y. The Parallel Fluorescence Determination of Iron(III), Terbium(III) and Europium(III) Ions Using the Coal-Derived Carbon Dot. Microchem. J. 2022, 177, 107255.
- 63. Xue, H.; Yan, Y.; Hou, Y.; Li, G.; Hao, C. Novel Carbon Quantum Dots for Fluorescent Detection of Phenol and Insights into the Mechanism. New J. Chem. 2018, 42 (14), 11485-11492.
- 64. Yew, Y. T.; Loo, A. H.; Sofer, Z.; Klímová, K.; Pumera, M. Coke-derived Graphene Quantum Dots as Fluorescence Nanoquencher in DNA Detection. Appl. Mater. Today 2017, 7, 138-143.
- 65. Saikia, M.; Hower, J. C.; Das, T.; Dutta, T.; Saikia, B. K. Feasibility Study of Preparation of Carbon Quantum Dots from Pennsylvania Anthracite and Kentucky Bituminous Coals. Fuel 2019, 243, 433-440.
- 66. Saikia, M.; Das, T.; Dihingia, N.; Fan, X.; Silva, L. F. O.; Saikia, B. K. Formation of Carbon Quantum Dots and Graphene Nanosheets from Different Abundant Carbonaceous Materials. Diam. Relat. Mater. 2020, 106, 107813.
- 67. Liu, M.; Li, X.; Zheng, Y.; Zhu, Y.; Li, T.; He, Z.; Zhang, C.; Zhang, K. Microwave-assisted Green Synthesis of Asphaltene-Based Carbon Dots for Micelle Sensitized Fluorescent Probes. J. Mater. Sci. 2023, 58
- 68. Hu, S.; Wei, Z.; Chang, Q.; Trinchi, A.; Yang, J. A Facile and Green Method towards Coal-Based Fluorescent Carbon Dots with Photocatalytic Activity. Appl. Surf. Sci. 2016, 378, 402-407.
- 69. Singamaneni, S. R.; van Tol, J.; Ye, R.; Tour, J. M. Intrinsic and Extrinsic Defects in a Family of Coal-Derived Graphene Quantum Dots. Appl. Phys. Lett. 2015, 107 (21), 212402.
- 70. Kundu, N.; Bhunia, P.; Sarkar, S.; Biswas, P. Highly Fluorescent Carbon Dots from Quinoline Insoluble Residues in Coal Tar. Opt. Mater. 2020,
- 71. Yeh, T.; Huang, W.; Chung, C.; Chiang, I.; Chen, L.; Chang, H.; Su, W. C.; Cheng, C.; Chen, S. J.; Teng, H. Elucidating Quantum Confinement in Graphene Oxide Dots Based on Excitationwavelength-independent Photoluminescence. J. Phys. Chem. Lett. **2016**, 7 (11), 2087-2092.
- 72. Cushing, S. K.; Li, M.; Huang, F.; Wu, N. Origin of Strong Excitation Wavelength Dependent Fluorescence of Graphene Oxide. ACS Nano 2014, 8 (1), 1002-1013.
- 73. Gan, Z.; Xiong, S.; Wu, X.; Xu, T.; Zhu, X.; Gan, X.; Guo, J.; Shen, J.; Sun, L.; Chu, P. K. Mechanism of Photoluminescence from Chemically Derived Graphene Oxide: Role of Chemical Reduction. Adv. Opt. Mater. 2013, 1
- 74. Feng, X.; Zhang, Y. A Simple and Green Synthesis of Carbon Quantum Dots from Coke for White Light-Emitting Devices. RSCAdv. 2019, 9 (58), 33789-33793.
- 75. Kundu, A.; Maity, B.; Basu, S. Coal-derived Graphene Quantum Dots with a Mn<sup>2+</sup>/Mn<sup>7+</sup> Nanosensor for Selective Detection of Glutathione by a Fluorescence Switch-Off-On Assay. New J. Chem. 2022, 46 (16),
- 76. Jia, J.; Sun, Y.; Zhang, Y.; Liu, Q.; Cao, J.; Huang, G.; Xing, B.; Zhang, C.; Zhang, L.; Cao, Y. Facile and Efficient Fabrication of Bandgap Tunable Carbon Quantum Dots Derived from Anthracite and Their Photoluminescence Properties. Front. Chem. 2020, 8; https://doi.org/ 10.3389/fchem.2020.00123.

- 77. Mathews, J. P.; Chaffee, A. L. The Molecular Representations of Coal -A Review. Fuel 2012, 96, 1-14.
- 78. Geng, B.; Yang, D.; Zheng, F.; Zhang, C.; Zhan, J.; Li, Z.; Pan, D.; Wang, L. Facile Conversion of Coal Tar to Orange Fluorescent Carbon Quantum Dots and Their Composite Encapsulated by Liposomes for Bioimaging. New J. Chem. 2017, 41 (23), 14444-14451.
- 79. Ye, R.; Peng, Z.; Metzger, A.; Lin, J.; Mann, J. A.; Huang, K.; Xiang, C.; Fan, X.; Samuel, E. L. G.; Alemany, L. B.; Martí, A. A.; Tour, J. M. Bandgap Engineering of Coal-Derived Graphene Quantum Dots. ACS Appl. Mater. Inter. 2015, 7 (12), 7041-7048.
- 80. Ye, R.; Xiang, C.; Lin, J.; Peng, Z.; Huang, K.; Yan, Z.; Cook, N. P.; Samuel, E. L. G.; Hwang, C. C.; Ruan, G.; Ceriotti, G.; Raji, A. R. O.; Martí, A. A.; Tour, J. M. Correction: Corrigendum: Coal as an Abundant Source of Graphene Quantum Dots. Nat. Commun. 2015, 6 (1), 2943.
- 81. Dong, Y.; Lin, J.; Chen, Y.; Fu, F.; Chi, Y.; Chen, G. Graphene Quantum Dots, Graphene Oxide, Carbon Quantum Dots and Graphite Nanocrystals in Coals. Nanoscale 2014, 6 (13), 7410-7415.
- 82. Li, R.; Tang, Y.; Che, Q.; Huan, X.; Ma, P.; Luo, P.; Mao, X. Study on the Microstructure of the Symbiosis of Coal-Based Graphene and Coal-Based Graphene Quantum Dots: Preparation and Characterization. Nanotechnology 2022, 33 (45), 455702.
- 83. Hu, C.; Yu, C.; Li, M.; Wang, X.; Yang, J.; Zhao, Z.; Eychmüller, A.; Sun, Y.; Qiu, J. Chemically Tailoring Coal to Fluorescent Carbon Dots with Tuned Size and Their Capacity for Cu(II) Detection. Small 2014, 10 (23), 4926-4933.
- 84. Zhang, Z.; Xu, X. Nondestructive Covalent Functionalization of Carbon Nanotubes by Selective Oxidation of the Original Defects with K2FeO4. Appl. Surf. Sci. 2015, 346, 520-527.
- 85. Peng, L.; Xu, Z.; Liu, Z.; Wei, Y.; Sun, H.; Li, Z.; Zhao, X.; Gao, C. An Iron-Based Green Approach to 1-h Production of Single-Layer Graphene Oxide. Nat. Commun. 2015, 6 (1), 5716.
- 86. Li, P.; Zong, Z.; Wei, X.; Wang, Y.; Fan, G. Structural Features of Liquefaction Residue from Shenmu-Fugu Subbituminous Coal. Fuel **2019**, 242, 819-827.
- 87. Wu, Z.; Rodgers, R. P.; Marshall, A. G. ESI FT-ICR Mass Spectral Analysis of Coal Liquefaction Products. Fuel 2005, 84 (14-15), 1790-1797.
- 88. Yang, J.; Wang, Z.; Liu, Z.; Zhang, Y. Novel Use of Residue from Direct Coal Liquefaction Process. Energ. Fuel. 2009, 23 (10), 4717–4722.
- 89. Khare, S.; Dell'Amico, M. An Overview of Conversion of Residues from Coal Liquefaction Processes. Can. J. Chem. Eng. 2013, 91 (10), 1660-1670.
- 90. Qin, F.; Li, Q.; Tang, T.; Zhu, J.; Gan, X.; Chen, Y.; Li, Y.; Zhang, S.; Huang, X.; Jia, D. Functional Carbon Dots from a Mild Oxidation of Coal Liquefaction Residue. Fuel 2022, 322, 124216.
- 91. Ghorai, S.; Roy, I.; De, S.; Dash, P. S.; Basu, A; Chattopadhyay, D. Exploration of the Potential Efficacy of Natural Resource-Derived Blue-Emitting Graphene Quantum Dots in Cancer Therapeutic Applications. New J. Chem. 2020, 44 (14), 5366-5376.
- 92. Shi, F.; Xing, B.; Zeng, H.; Guo, H.; Qu, X.; Huang, G.; Cao, Y.; Li, P.; Zhang, C. Ice Template Induced Assembly Strategy for Preparation of 3D Porous Carbon Frameworks from Low-Cost Carbon Quantum Dots for High-Performance Lithium-Ion Batteries. J. Energy Storage 2023, 70, 107982.
- 93. Liu, Q.; Zhang, J.; He, H.; Huang, G.; Xing, B.; Jia, J.; Zhang, C. Green Preparation of High Yield Fluorescent Graphene Quantum Dots from Coal-Tar-Pitch by Mild Oxidation. Nanomaterials 2018, 8 (10), 844.
- 94. Bai, J.; Xiao, N.; Wang, Y.; Li, H.; Liu, C.; Xiao, J.; Wei, Y.; Guo, Z.; Qiu, J. Coal Tar Pitch Derived Nitrogen-Doped Carbon Dots with Adjustable Particle Size for Photocatalytic Hydrogen Generation. Carbon 2021, 174, 750-756.

- 95. Kang, S.; Kim, K. M.; Jung, K.; Son, Y.; Mhin, S.; Ryu, J. H.; Shim, K. B.; Lee, B.; Han, H.; Song, T. Publisher Correction: Graphene Oxide Quantum Dots Derived from Coal for Bioimaging: Facile and Green Approach. Sci. Rep.-UK 2020, 10 (1), 7451.
- 96. Ran, Q.; Wang, X.; Ling, P.; Yan, P.; Xu, J.; Jiang, L.; Wang, Y.; Su, S.; Hu, S.; Xiang, J. A Thermal-Assisted Electrochemical Strategy to Synthesize Carbon Dots with Bimodal Photoluminescence Emission. Carbon 2022, 193, 404-411.
- 97. He, M.; Guo, X.; Huang, J.; Shen, H.; Zeng, Q.; Wang, L. Mass Production of Tunable Multicolor Graphene Quantum Dots from an Energy Resource of Coke by a One-step Electrochemical Exfoliation. Carbon 2018, 140, 508-520.
- 98. Zhou, X.; Zhang, Y.; Wang, C.; Wu, X.; Yang, Y.; Zheng, B.; Wu, H.; Guo, S.; Zhang, J. Photo-Fenton Reaction of Graphene Oxide: A New Strategy to Prepare Graphene Quantum Dots for DNA Cleavage. ACS Nano 2012, 6 (8), 6592-6599.
- 99. Sasikala, S. P.; Henry, L.; Yesilbag Tonga, G.; Huang, K.; Das, R.; Giroire, B.; Marre, S.; Rotello, V. M.; Penicaud, A.; Poulin, P.; Aymonier, C. High Yield Synthesis of Aspect Ratio Controlled Graphenic Materials from Anthracite Coal in Supercritical Fluids. ACS Nano 2016, 10 (5), 5293-5303.
- 100. Brunner, G. Near Critical and Supercritical Water. Part I. Hydrolytic and Hydrothermal Processes. J. Supercrit. Fluids 2009, 47 (3), 373-381.
- 101. Zhang, J.; Zhao, S. S.; Yang, Z.; Yang, Z.; Yang, S.; Liu, X. Hydrothermal Synthesis of Blue-green Emitting Carbon Dots Based on the Liquid Products of Biodegradation of Coal. Int. J. Energ. Res. 2021, 45 (6), 9396-9407.
- 102. Kumar Thiyagarajan, S.; Raghupathy, S.; Palanivel, D.; Raji, K.; Ramamurthy, P. Fluorescent Carbon Nano Dots from Lignite: Unveiling the Impeccable Evidence for Quantum Confinement. Phys. Chem. Chem. Phys. 2016, 18 (17), 12065-12073.
- 103. Zhang, Y.; Li, K.; Ren, S.; Dang, Y.; Liu, G.; Zhang, R.; Zhang, K.; Long, X.; Jia, K. Coal-Derived Graphene Quantum Dots Produced by Ultrasonic Physical Tailoring and Their Capacity for Cu(II) Detection. ACS Sustain. Chem. Eng. 2019, 7 (11), 9793-9799.
- 104. Das, T.; Saikia, B. K.; Dekaboruah, H. P.; Bordoloi, M.; Neog, D.; Bora, J. J.; Lahkar, J.; Narzary, B.; Roy, S.; Ramaiah, D. Blue-fluorescent and Biocompatible Carbon Dots Derived from Abundant Low-Quality Coals. J. Photochem. Photobiol. B Biol. 2019, 195, 1–11.
- 105. Lueking, A. D.; Gutierrez, H. R.; Fonseca, D. A.; Narayanan, D. L.; Van Essendelft, D.; Jain, P.; Clifford, C. E. B. Combined Hydrogen Production and Storage with Subsequent Carbon Crystallization. J. Am. Chem. Soc. 2006, 128 (24), 7758-7760.
- 106. Lueking, A. D.; Gutierrez, H. R.; Jain, P.; Van Essandelft, D. T.; Burgess-Clifford, C. E. The Effect of HCl and NaOH Treatment on Structural Transformations in a Ball-Milled Anthracite after Thermal and Chemical Processing. Carbon 2007, 45 (11), 2297-2306.
- 107. Sun, Y.; Kvashnin, A. G.; Sorokin, P. B.; Yakobson, B. I.; Billups, W. E. Radiation-Induced Nucleation of Diamond from Amorphous Carbon: Effect of Hydrogen. J. Phys. Chem. Lett. 2014, 5 (11), 1924-1928.
- 108. Yang, G. W. Laser Ablation in Liquids: Applications in the Synthesis of Nanocrystals. Prog. Mater. Sci. 2007, 52 (4), 648-698.
- 109. Nigam, P.; Waghmode, S.; Louis, M.; Wangnoo, S.; Chavan, P.; Sarkar, D. Graphene Quantum Dots Conjugated Albumin Nanoparticles for Targeted Drug Delivery and Imaging of Pancreatic Cancer. J. Mater. Chem. B 2014, 2 (21), 3190-3195.
- 110. Nirala, N. R.; Khandelwal, G.; Kumar, B.; Vinita, P. R.; Kumar, V. One Step Electro-Oxidative Preparation of Graphene Quantum Dots from Wood Charcoal as a Peroxidase Mimetic. Talanta 2017, 173, 36-43.

- 111. Seel, J. A.; Dahn, J. R. Electrochemical Intercalation of PF<sub>6</sub> into Graphite. J. Electrochem. Soc. 2000, 147 (3), 892-898.
- 112. Katinonkul, W.; Lerner, M. M. Graphite Intercalation Compounds with Large Fluoroanions. J Fluorine Chem. 2007, 128 (4), 332-335.
- 113. Li, Z.; Zhang, W.; Luo, Y.; Yang, J.; Hou, J. G. How Graphene Is Cut upon Oxidation? J. Am. Chem. Soc. 2009, 131 (18), 6320-6321.
- 114. Li, J. L.; Kudin, K. N.; McAllister, M. J.; Prud'Homme, R. K.; Aksay, I. A.; Car, R. Oxygen-driven Unzipping of Graphitic Materials. Phys. Rev. Lett. 2006, 96 (17), 176101.
- 115. Yu, X.; Liu, X.; Jiang, Y.; Li, Y.; Gao, G.; Zhu, Y.; Lin, F.; Wu, F. G. Rose Bengal-Derived Ultrabright Sulfur-Doped Carbon Dots for Fast Discrimination between Live and Dead Cells. Anal. Chem. 2022, 94 (10),
- 116. Wu, S.; Zhou, R.; Chen, H.; Zhang, J.; Wu, P. Highly Efficient Oxygen Photosensitization of Carbon Dots: the Role of Nitrogen Doping. Nanoscale 2020, 12 (9), 5543-5553.
- 117. Hu, S.; Meng, X.; Tian, F.; Yang, W.; Li, N.; Xue, C.; Yang, J.; Chang, Q. Dual Photoluminescence Centers from Inorganic-Salt-Functionalized Carbon Dots for Ratiometric pH Sensing. J. Mater. Chem. C 2017, 5 (38), 9849-9853.
- 118. Zhu, S.; Meng, Q.; Wang, L.; Zhang, J.; Song, Y.; Jin, H.; Zhang, K.; Sun, H.; Wang, H.; Yang, B. Highly Photoluminescent Carbon Dots for Multicolor Patterning, Sensors, and Bioimaging. Angew. Chem. Int. Ed. **2013**, *52* (14), 3953–3957.
- 119. Saikia, M.; Das, T.; Saikia, B. K. A Novel Rapid Synthesis of Highly Stable Silver Nanoparticle/carbon Quantum Dot Nanocomposites Derived from Low-Grade Coal Feedstock. New J. Chem. 2021, 46 (1),
- 120. Hu, Q.; Yang, X.; Qi, Y.; Wei, P.; Cheng, J.; Xie, Y. Optimization of Perovskite/carbon Interface Performance Using N-Doped Coal-Based Graphene Quantum Dots and its Mechanism Analysis. J. Energy Chem. **2023**, 79, 242-252.
- 121. Sun, J.; Maimaiti, H.; Xu, B.; Feng, L.; Bao, J.; Zhao, X. Photoelectrocatalytic Degradation of Wastewater and Simultaneous Hydrogen Production on Copper Nanorod-Supported Coal-Based N-Carbon Dot Composite Nanocatalysts. Appl. Surf. Sci. 2022, 585, 152701.
- 122. Li, M.; Hu, C.; Yu, C.; Wang, S.; Zhang, P.; Qiu, J. Organic Amine-Grafted Carbon Quantum Dots with Tailored Surface and Enhanced Photoluminescence Properties. Carbon 2015, 91, 291-297.
- 123. Nilewski, L.; Mendoza, K.; Jalilov, A. S.; Berka, V.; Wu, G.; Sikkema, W. K. A.; Metzger, A.; Ye, R.; Zhang, R.; Luong, D. X.; Wang, T.; McHugh, E.; Derry, P. J.; Samuel, E. L.; Kent, T. A.; Tsai, A. L.; Tour, J. M. Highly Oxidized Graphene Quantum Dots from Coal as Efficient Antioxidants. ACS Appl. Mater. Inter. 2019, 11 (18), 16815-16821.
- 124. Sun, F.; Maimaiti, H.; Liu, Y.; Awati, A. Preparation and Photocatalytic CO<sub>2</sub> Reduction Performance of Silver Nanoparticles Coated with Coal-Based Carbon Dots. Int. J. Energ. Res. 2018, 42 (14), 4458-4469.
- 125. Han, X.; Han, Y.; Huang, H.; Zhang, H.; Zhang, X.; Liu, R.; Liu, Y.; Kang, Z. Synthesis of Carbon Quantum dots/SiO<sub>2</sub> Porous Nanocomposites and Their Catalytic Ability for Photo-Enhanced Hydrocarbon Selective Oxidation. Dalton T 2013, 42 (29), 10380.
- 126. Chan, K. T.; Neaton, J. B.; Cohen, M. L. First-principles Study of Metal Adatom Adsorption on Graphene. Phys. Rev. B Condens. Matter. 2008,
- 127. Hu, C.; Zhu, Y.; Zhao, X. On-off-on Nanosensors of Carbon Quantum Dots Derived from Coal Tar Pitch for the Detection of Cu<sup>2+</sup>, Fe<sup>3+</sup>, and L-Ascorbic Acid. Spectrochim. Acta Mol. Biomol. Spectrosc. 2021, 250, 119325.

- 128. Zhang, S.; Yan, H.; Li, H.; Xu, T.; Li, H.; Wang, C.; Yang, Z.; Jia, X.; Liu, X. Carbon Dots as Specific Fluorescent Sensors for Hg<sup>2+</sup> and Glutathione Imaging. Microchim. Acta 2023, 190 (6), 224.
- 129. Li, M.; Yu, C.; Hu, C.; Yang, W.; Zhao, C.; Wang, S.; Zhang, M.; Zhao, J.; Wang, X.; Qiu, J. Solvothermal Conversion of Coal into Nitrogen-Doped Carbon Dots with Singlet Oxygen Generation and High Quantum Yield. Chem. Eng. J. (Lausanne, Switzerland: 1996) 2017, 320, 570-575.
- 130. Hu, C.; Yu, C.; Li, M.; Wang, X.; Dong, Q.; Wang, G.; Qiu, J. Nitrogendoped Carbon Dots Decorated on Graphene: a Novel All-Carbon Hybrid Electrocatalyst for Enhanced Oxygen Reduction Reaction. Chem. Commun. 2015, 51 (16), 3419-3422.
- 131. Fei, H.; Ye, R.; Ye, G.; Gong, Y.; Peng, Z.; Fan, X.; Samuel, E. L. G.; Ajayan, P. M.; Tour, J. M. Boron- and Nitrogen-Doped Graphene Quantum Dots/Graphene Hybrid Nanoplatelets as Efficient Electrocatalysts for Oxygen Reduction. ACS Nano 2014, 8 (10), 10837-10843.
- 132. Su, Y.; Zhang, Y.; Zhuang, X.; Li, S.; Wu, D.; Zhang, F.; Feng, X. Lowtemperature Synthesis of Nitrogen/sulfur Co-doped Three-Dimensional Graphene Frameworks as Efficient Metal-free Electrocatalyst for Oxygen Reduction Reaction. Carbon 2013, 62, 296-301.
- 133. Li, Z.; Li, Y.; Wang, L.; Cao, L.; Liu, X.; Chen, Z.; Pan, D.; Wu, M. Assembling Nitrogen and Oxygen Co-doped Graphene Quantum Dots onto Hierarchical Carbon Networks for All-Solid-State Flexible Supercapacitors. Electrochim. Acta 2017, 235, 561-569.
- 134. Qu, A.; Xie, H.; Xu, X.; Zhang, Y.; Wen, S.; Cui, Y. High Quantum Yield Graphene Quantum Dots Decorated TiO<sub>2</sub> Nanotubes for Enhancing Photocatalytic Activity. Appl. Surf. Sci. 2016, 375, 230-241.
- 135. Ananthanarayanan, A.; Wang, Y.; Routh, P.; Sk, M. A.; Than, A.; Lin, M.; Zhang, J.; Chen, J.; Sun, H.; Chen, P. Nitrogen and Phosphorus Codoped Graphene Quantum Dots: Synthesis from Adenosine Triphosphate, Optical Properties, and Cellular Imaging. Nanoscale **2015**, 7 (17), 8159-8165.
- 136. Xu, Y.; Wang, S.; Hou, X.; Sun, Z.; Jiang, Y.; Dong, Z.; Tao, Q.; Man, J.; Cao, Y. Coal-derived Nitrogen, Phosphorus and Sulfur Co-doped Graphene Quantum Dots: A Promising Ion Fluorescent Probe. Appl. Surf. Sci. 2018, 445, 519-526.
- 137. Chimeno-Trinchet, C.; Pacheco, M. E.; Fernández-González, A.; Badía-Laíño, R. Modified Lanthanide-Doped Carbon Dots as a Novel Nanochemosensor for Efficient Detection of Water in Toluene and its Potential Application in Lubricant Base Oils. Microchim. Acta 2023, 190 (3), 97.
- 138. Li, M; Chen, T.; Gooding, J. J.; Liu, J. Review of Carbon and Graphene Quantum Dots for Sensing. ACS Sens. 2019, 4 (7), 1732-1748.
- 139. Sun, H.; Wu, L.; Wei, W.; Qu, X. Recent Advances in Graphene Quantum Dots for Sensing. Mater. Today 2013, 16 (11), 433-442.
- 140. Sun, X.; He, J.; Meng, Y.; Zhang, L.; Zhang, S.; Ma, X.; Dey, S.; Zhao, J.; Lei, Y. Microwave-assisted Ultrafast and Facile Synthesis of Fluorescent Carbon Nanoparticles from a Single Precursor: Preparation, Characterization and Their Application for the Highly Selective Detection of Explosive Picric Acid. J. Mater. Chem. A. 2016, 4 (11), 4161-4171.
- 141. Wang, B.; Mu, Y.; Zhang, C.; Li, J. Blue Photoluminescent Carbon Nanodots Prepared from Zeolite as Efficient Sensors for Picric Acid Detection. Sensor. Actuator. B Chem. 2017, 253, 911-917.
- 142. Wang, C.; Xu, Z.; Cheng, H.; Lin, H.; Humphrey, M. G.; Zhang, C. A Hydrothermal Route to Water-Stable Luminescent Carbon Dots as Nanosensors for pH and Temperature. Carbon 2015, 82, 87-95.
- 143. Hu, Y.; Yang, J.; Jia, L.; Yu, J. Ethanol in Aqueous Hydrogen Peroxide Solution: Hydrothermal Synthesis of Highly Photoluminescent

- Carbon Dots as Multifunctional Nanosensors. Carbon 2015, 93, 999-1007.
- 144. Zhang, H.; Abdiryim, T.; Jamal, R.; Liu, X.; Niyaz, M.; Xie, S.; Liu, H.; Kadir, A.; Serkjan, N. Coal-based Carbon Quantum Dots-Sensitized TiO<sub>2</sub> NRs/PTTh Heterostructure for Self-Powered UV Detection. Appl. Surf. Sci. 2022, 605, 154797.
- 145. Yu, J.; Zhang, C.; Yang, Y.; Yi, G.; Fan, R.; Li, L.; Xing, B.; Liu, Q.; Jia, J.; Huang, G. Lignite-Derived Carbon Quantum dot/TiO<sub>2</sub> Heterostructure Nanocomposites: Photoinduced Charge Transfer Properties and Enhanced Visible Light Photocatalytic Activity. New J. Chem. 2019, 43 (46), 18355-18368,
- 146. Zhang, B.; Maimaiti, H.; Zhang, D.; Xu, B.; Wei, M. Preparation of Coal-Based C-Dots/TiO<sub>2</sub> and its Visible-Light Photocatalytic Characteristics for Degradation of Pulping Black Liquor. J. Photochem. Photobiol. Chem. 2017, 345, 54-62.
- 147. Hu, S.; Ding, Y.; Chang, Q.; Yang, J.; Lin, K. Chlorine-functionalized Carbon Dots for Highly Efficient Photodegradation of Pollutants under Visible-Light Irradiation. Appl. Surf. Sci. 2015, 355, 774-777.
- 148. Hu, S.; Zhang, W.; Chang, Q.; Yang, J.; Lin, K. A Chemical Method for Identifying the Photocatalytic Active Sites on Carbon Dots. Carbon 2016, 103, 391-393.
- 149. Zhao, S.; Li, C.; Wang, L.; Liu, N.; Qiao, S.; Liu, B.; Huang, H.; Liu, Y.; Kang, Z. Carbon Quantum Dots Modified MoS<sub>2</sub> with Visible-Light-Induced High Hydrogen Evolution Catalytic Ability. Carbon 2016, 99, 599-606.
- 150. Tian, L.; Li, Z.; Wang, P.; Zhai, X.; Wang, X.; Li, T. Carbon Quantum Dots for Advanced Electrocatalysis. J. Energy Chem. 2021, 55, 279-294.
- 151. Luo, Y.; Liu, Y.; Wu, L.; Ma, X.; Liu, Q.; Huang, F.; Zhang, X.; Zhang, Y.; Zhang, J.; Luo, H.; Yang, Y.; Lu, G.; Tang, X.; Li, L.; Zeng, Y.; Pan, T.; Zhang, H. CUL<sub>7</sub>E<sub>3</sub> Ubiquitin Ligase Mediates the Degradation of Activation-Induced Cytidine Deaminase and Regulates the Iq Class Switch Recombination in B Lymphocytes. J. Immunol. 2019, 203 (1), 269-281.
- 152. Muthurasu, A.; Maruthapandian, V.; Kim, H. Y. Metal-organic Framework Derived Co<sub>3</sub>O<sub>4</sub>/MoS<sub>2</sub> Heterostructure for Efficient Bifunctional Electrocatalysts for Oxygen Evolution Reaction and Hydrogen Evolution Reaction. Appl. Catal. B Environ. 2019, 248, 202-210.
- 153. Xu, H.; Shang, H.; Wang, C.; Jin, L.; Chen, C.; Wang, C.; Du, Y. Threedimensional Open CoMoO<sub>x</sub>/CoMoS<sub>x</sub>/CoS<sub>x</sub> Nanobox Electrocatalysts for Efficient Oxygen Evolution Reaction. Appl. Catal. B Environ. 2020,
- 154. Sebastián, D.; Serov, A.; Matanovic, I.; Artyushkova, K.; Atanassov, P.; Aricò, A. S.; Baglio, V. Insights on the Extraordinary Tolerance to Alcohols of Fe-N-C Cathode Catalysts in Highly Performing Direct Alcohol Fuel Cells. Nano Energy 2017, 34, 195-204.
- 155. Zhao, H.; Ma, M.; Dai, P.; Jing, W.; Yin, D.; Li, X.; Xing, H.; Ali, W.; Ali Khan, N.; Li, P.; Fan, X.; Ding, S. Bottom-up Synthesis of Highly Active Catalyst by Coal-Derived Carbon Quantum Dots for Oxygen Evolution Reaction. Mater. Lett. 2022, 322, 132470.
- 156. Kovalchuk, A.; Huang, K.; Xiang, C.; Martí, A. A.; Tour, J. M. Luminescent Polymer Composite Films Containing Coal-Derived Graphene Quantum Dots. ACS Appl. Mater. Inter. 2015, 7 (47), 26063–26068.
- 157. Li, H.; Yuan, D.; Tang, C.; Wang, S.; Sun, J.; Li, Z.; Tang, T.; Wang, F.; Gong, H.; He, C. Lignin-derived Interconnected Hierarchical Porous Carbon Monolith with Large Areal/volumetric Capacitances for Supercapacitor. Carbon 2016, 100, 151-157.
- Luo, X.; Chen, Y.; Mo, Y. A Review of Charge Storage in Porous Carbon-158. Based Supercapacitors. New Carbon Mater. 2021, 36 (1), 49-68.

- 159. Zhang, S.; Zhu, J.; Qing, Y.; Fan, C.; Wang, L.; Huang, Y.; Sheng, R.; Guo, Y.; Wang, T.; Pan, Y.; Lv, Y.; Song, H.; Jia, D. Construction of Hierarchical Porous Carbon Nanosheets from Template-Assisted Assembly of Coal-Based Graphene Quantum Dots for High Performance Supercapacitor Electrodes. Mater. Today Energy **2017**, 6, 36-45.
- 160. Shi, F.; Liu, Q.; Zhang, J.; Xing, B.; Huang, G.; Jia, J.; Zhang, C. One-Pot Synthesis of an FeS@GQDs Composite for Lithium Storage with Coal Tar Pitch as "Natural GQDs. Energ. Fuel 2022, 36 (4), 2130-2139.
- 161. Zhang, Y.; Zhang, K.; Jia, K.; Liu, G.; Ren, S.; Li, K.; Long, X.; Li, M.; Qiu, J. Preparation of Coal-Based Graphene Quantum Dots/α-Fe<sub>2</sub>O<sub>3</sub> Nanocomposites and Their Lithium-Ion Storage Properties. Fuel 2019, 241, 646-652.
- 162. Zhang, L.; Aboagye, A.; Kelkar, A.; Lai, C.; Fong, H. A Review: Carbon Nanofibers from Electrospun Polyacrylonitrile and Their Applications. J. Mater. Sci. 2014, 49 (2), 463-480.
- 163. Lu, X.; Wang, C.; Favier, F.; Pinna, N. Electrospun Nanomaterials for Supercapacitor Electrodes: Designed Architectures and Electrochemical Performance. Adv. Energy Mater. 2017, 7 (2), 1601301.
- 164. Peng, S.; Jin, G.; Li, L.; Li, K.; Srinivasan, M.; Ramakrishna, S.; Chen, J. Multi-functional Electrospun Nanofibres for Advances in Tissue Regeneration, Energy Conversion & Storage, and Water Treatment. Chem. Soc. Rev. 2016, 45 (5), 1225-1241.
- 165. Zhu, J.; Zhang, S.; Wang, L.; Jia, D.; Xu, M.; Zhao, Z.; Qiu, J. Engineering Cross-Linking by Coal-Based Graphene Quantum Dots toward Tough, Flexible, and Hydrophobic Electrospun Carbon Nanofiber Fabrics. Carbon 2018, 129, 54-62.